อภินันทนาการ

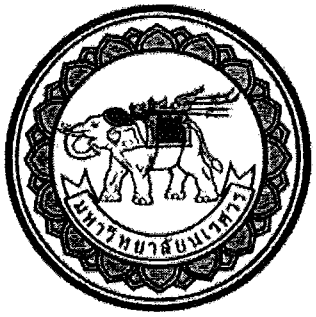

รายงานวิจัยฉบับสมบูรณ์

อนุภาคนาโนแม่เหล็กเคลือบด้วยพอลิเมอร์แบบแอมฟิไฟล์สองชั้นเพื่อการปลดปล่อยยาแบบต่อเนื่อง

Synthesis of magnetic nanoparticle coated with amphiphilic polymeric bilayer for sustained drug release

โดย รองศาสตราจารย์ ดร. เมธา รัตนากรพิทักษ์

สิงหาคม 2561

สัญญาเลขที่ R2561B086

รายงานวิจัยฉบับสมบูรณ์

อนุภาคนาโนแม่เหล็กเคลือบด้วยพอลิเมอร์แบบแอมฟิไฟล์สองชั้นเพื่อการปลดปล่อยยาแบบต่อเนื่อง

Synthesis of magnetic nanoparticle coated with amphiphilic polymeric bilayer for sustained drug release or poly(ethylene glycol)

โดย

รองศาสตราจารย์ ดร.เมธา รัตนากรพิทักษ์
ภาควิชาเคมี คณะวิทยาศาสตร์ มหาวิทยาลัยนเรศวร

สนับสนุนโดยงบประมาณแผ่นดิน ประจำปี 2561 มหาวิทยาลัยนเรศวร

ACKNOWLEDGEMENT

The authors acknowledge The National Research Council of Thailand (NRCT) (R2561B086) for financial support of this work.

บทสรุปผู้บริหาร
(Executive summary)

งานวิจัยนี้ศึกษาการสังเคราะห์พอลิเมอร์ร่วมระหว่างพอลิเอ็นเอ็นไดเอทิลอะมิโนเอทิลเมทาคริเลทบล็อกพอลิเอ็นโซโพรพิลอะคริลาไมด์-ไธโอแลคโทนอะคริลาไมด์ (PDEAEMA-*b*-P(NIPAAm-*st*-TlaAm) copolymer) เพื่อใช้ในการเคลือบพื้นผิวของอนุภาคนาโนแมกนีไทท์แบบสองชั้นและเพื่อเหนี่ยวนำให้เกิดการเกาะกลุ่มของอนุภาคแบบที่ควบคุมได้ นอกจากนี้ ยังได้ศึกษาการประยุกต์ใช้อนุภาคนี้ในการดักจับยาเพื่อควบคุมการปลดปล่อยยาและการตรึงสารชีวโมเลกุล โดยหน่วย TlaAm ของวงไธโอแลคโทนที่เคลือบบนพื้นผิวอนุภาคสามารถเกิดปฏิกิริยาการเปิดวงด้วยหมู่เอมีนของสารอัลคิลเอมีน และเกิดเป็นหมู่ฟังก์ชันไธออล (-SH) ตามด้วยปฏิกิริยาไธออล-อีน กับหมู่ฟังก์ชันอะคริลาไมด์ที่ถูกตรึงอยู่บนพื้นผิวของอนุภาคนาโนแมกนีไทท์ จากนั้นเมื่อทำปฏิกิริยาการควอเทอไนเซชันแล้ว จะทำให้ได้อนุภาคที่มีประจุบวกบนพื้นผิว ซึ่งสามารถเหนี่ยวนำให้เกิดเป็นนาโนคลัสเตอร์ที่มีขนาดเส้นผ่าศูนย์กลางน้อยกว่า 200 นาโนเมตร ในปฏิกิริยาการเปิดวงไธโอแลคโทนนั้น ได้ใช้สารอัลคิลเอมีนหลายชนิดในการทำปฏิกิกิริยาเปิดวง ทั้งนี้เพื่อต้องการศึกษาผลของความยาวของหมู่อัลคิลที่แตกต่างกัน (ได้แก่ 1-โพรพิลเอมีน (C3) 1-ออกทิลเอมีน (C8) หรือ 1-โดเดกซิลเอมีน (C12)) และระดับความเป็นขั้วที่แตกต่างกัน ต่อความสามารถในการตอบสนองต่อสนามแม่เหล็ก ความสามารถในการกระจายตัวในน้ำและอัตราการปลดปล่อยยาต้นแบบ (งานวิจัยนี้ใช้ยาอินโดเมทาซินเป็นยาต้นแบบ) จากผลการศึกษาพบว่า เมื่อเพิ่มอุณหภูมิของสารละลาย จะมีผลต่อลักษณะการรวมกลุ่มของอนุภาคนาโน โดยจะทำให้ขนาดไฮโดรไดนามิกลดลงและอัตราการปลดปล่อยยาเพิ่มมากขึ้น ซึ่งแสดงถึงว่าอนุภาคนาโนแมกนีไทท์ที่มีการเคลือบด้วยพอลิเมอร์ร่วมชนิดใหม่นี้ น่าจะสามารถนำไปประยุกต์ใช้เป็นวัสดุดูดจับยาที่มีกลไกการกระตุ้นการปลดปล่อยยาได้และอาจจะนำไปใช้เป็นตัวดูดจับสารชีวโมเลกุลอื่นๆหรือยาชนิดอื่นๆที่มีประจุลบได้ด้วย

ABSTRACT

This work presents the synthesis of magnetite nanoparticle (MNP) coated with poly(N,N-diethylaminoethyl methacrylate)-*b*-poly(N-isopropyl acrylamide-*st*-thiolactone acrylamide) (PDEAEMA-*b*-P(NIPAAm-*st*-TlaAm) copolymer and its use in controlled drug release and bio-conjugation. TlaAm units in the copolymer were ring-opened with various alkyl amines to form thiol groups (-SH), followed by thiol-ene coupling reactions with acrylamide-coated MNP and then quaternized to obtain cationic copolymer-MNP assemblies (the size < 200 nm/cluster). The use of alkyl amines having various chain lengths (e.g. 1-propylamine, 1-octylamine or 1-dodecylamine) in the nucleophilic ring-opening reactions of the thiolactone rings affected their magnetic separation ability, water dispersibility and release rate of doxorubicin model drug. In all cases, when increasing the temperature, they showed a thermo-responsive behavior as indicated by the decrease in hydrodynamic size and the accelerated drug release rate. These copolymer-MNP assemblies could be used as a novel platform with thermal-triggering controlled drug release and capability for adsorption with any negatively charged biomolecules.

บทคัดย่อ

งานวิจัยนี้ศึกษาการสังเคราะห์อนุภาคนาโนแมกนีไทท์ที่เคลือบด้วยพอลิเมอร์ร่วมระหว่างพอลิเอ็นเอ็นไดเอทิลอะมิโนเอทิลเมทาคริเลทบล็อกพอลิเอ็นโซโพรพิลอะคริลาไมด์-ไธโอแลคโทนอะคริลาไมด์ (PDEAEMA-*b*-P(NIPAAm-*st*-TlaAm) copolymer) เพื่อเกิดเป็นอนุภาคแม่เหล็กที่มีพอลิเมอร์เคลือบแบบสองชั้น โดยได้ศึกษาการประยุกต์ใช้อนุภาคนี้ในการดักจับยาเพื่อควบคุมการปลดปล่อยยาและการตรึงสารชีวโมเลกุล โดยหน่วย TlaAm ของวงไธโอแลคโทนที่เคลือบบนพื้นผิวอนุภาคสามารถเกิดปฏิกิริยาการเปิดวงด้วยหมู่เอมีนของสารอัลคิลเอมีน และเกิดเป็นหมู่ฟังก์ชันไธออล (-SH) ตามด้วยปฏิกิริยาไธออล-อีน กับหมู่ฟังก์ชันอะคริลาไมด์ที่ถูกตรึงอยู่บนพื้นผิวของอนุภาคนาโนแมกนีไทท์ จากนั้นเมื่อทำปฏิกิริยาการควอเทอไนเซชันแล้ว จะทำให้ได้อนุภาคที่มีประจุบวกบนพื้นผิว ซึ่งสามารถเหนี่ยวนำให้เกิดเป็นนาโนคลัสเตอร์ที่มีขนาดเส้นผ่าศูนย์กลางน้อยกว่า 200 นาโนเมตร ในปฏิกิริยาการเปิดวงไธโอแลคโทนนั้น ได้ใช้สารอัลคิลเอมีนหลายชนิดในการทำปฏิกิริยาเปิดวง ทั้งนี้เพื่อต้องการศึกษาผลของความยาวของหมู่อัลคิลที่แตกต่างกัน (ได้แก่ 1-โพรพิลเอมีน (C3) 1-ออกทิลเอมีน (C8) หรือ 1-โดเดกซิลเอมีน (C12)) และระดับความเป็นขั้วที่แตกต่างกัน ต่อความสามารถในการตอบสนองต่อสนามแม่เหล็ก ความสามารถในการกระจายตัวในน้ำและอัตราการปลดปล่อยยาต้นแบบ (งานวิจัยนี้ใช้ยาอินโดเมทาซินเป็นยาต้นแบบ) จากผลการศึกษาพบว่า เมื่อเพิ่มอุณหภูมิของสารละลายจะมีผลต่อลักษณะการรวมกลุ่มของอนุภาคนาโน โดยจะทำให้ขนาดไฮโดรไดนามิกลดลงและอัตราการปลดปล่อยยาเพิ่มมากขึ้น ซึ่งแสดงถึงว่าอนุภาคนาโนแมกนีไทท์ที่มีการเคลือบด้วยพอลิเมอร์ร่วมชนิดใหม่นี้ น่าจะสามารถนำไปประยุกต์ใช้เป็นวัสดุดูดจับยาที่มีกลไกการกระตุ้นการปลดปล่อยยาได้และอาจจะนำไปใช้เป็นตัวดูดจับสารชีวโมเลกุลอื่นๆหรือยาชนิดอื่นๆที่มีประจุลบได้ด้วย

LIST OF CONTENTS

CHAPTER I

INTRODUCTION

Research rationale

In recent years, magnetite nanoparticle (MNP) has extensively attracted interest owing to their superparamagnetic properties and their potential applications in various fields. Incorporation of MNP into various organic nano-assemblies has been investigated by features of their intriguing biomedical applications, such as remotely controlled drug release, magnetically guidable drug delivery [1-3], magnetic resonance imaging (MRI) [4-5], and hyperthermia cancer treatment [6-8]. However, it tends to aggregate to each other mainly owing to dipole-dipole and magnetic attractive forces, leading the loss in nano-scale related properties and a decrease in the surface area/volume ratio [9]. Grafting long-chain polymers onto MNP surface is currently one of the promising approaches to realize its dispersibility in the media due to charge repulsion of ionic surface or steric repulsion of long chain surfactant [10,11]. In addition, this polymeric coating can also serve as a platform for conjugation of biomolecules of interest on the MNP surface [12-15].

Many works have now extensively reported in the MNP polymeric coating accomplished either *via* "grafting from" or "grafting to" strategies [16,17] with controlled radical polymerization (CRP) techniques. CRP technique produces well controllable polymer architecture on particle surface because it can control molecular weight, polydispersity, functionality and composition distribution of polymers [18,19]. Three general techniques of CRP include nitroxide-mediated polymerization (NMP) [20,21], atom transfer radical polymerization (ATRP) [22,23], reversible addition fragmentation chain transfer polymerization (RAFT) [24,25]. Being of our particular interest, RAFT as opposed to other CRP techniques can be performed in various kinds of solvent, wide range of temperature, no need of metals used for polymerization and large range of monomer classes [26].

This present work reports the synthesis of a multifunctional amphiphilic copolymer with bilayer *via* RAFT for coating onto the surface of MNP and its use in drug controlled and sustained release and bio-conjugation. This copolymer was well designed to have multi-functions including; 1) thermo-responsive poly(N-isopropylacrylamide) (PNIPAAm) serving as a drug reservoir with a temperature-triggering mechanism for controlled and sustained release, 2) thiolactone moiety for covalent grafting with MNP surface and tuning degree of hydrophobicity of the copolymer, and 3) positively charged poly(N,N-diethylamino-2-ethylmethacrylate) (PDEAEMA) for improving its water dispersibility and ionic adsorption with anionic bio-entities. PNIPAAm responded to the change of the environmental temperature due to the phase separation when crossing its lower critical solution temperature (LCST = 30-34 °C) [27]. When raising the temperature above its LCST, the copolymer was in the collapse state due to the formation of the intramolecular hydrogen bonding among the polymer chains. In contrast, it swelled at the temperature below its LCST owing to the intermolecular hydrogen bonding between water molecules and polymer chains [28-32].

The reactions involving thiol chemistry has now gain a great attention because thiols (-SH) are highly reactive nucleophiles for the reactions with epoxide, alkyl halides, and double or triple bonds [33-34]. However, the applications of thiols are rather limited because they have a short shelf life due to the oxidation reaction resulting in disulfide formation [35]. A promising approach to overcome this limitation is to use a reactive thiolactone, a cyclic thioester, as a latent thiol functional group. This reaction involves a ring-opening reaction of thiolactone moieties to obtain thiol functionality (-SH), subsequently reacting with electrophiles for the second modification in one-pot reaction [33,36-38]. Many works from Du Prez's research group have reported the use of thiolactone for the double modification purpose [33-38].

In this report, we describe a synthesis of a thermo-responsive multifunctional diblock copolymer containing thiolactone acrylamide (TlaAm) units for coating on MNP surface and its use for drug controlled release and bio-conjugation applications. PDEAEMA synthesized *via* RAFT polymerization was used as a macro chain transfer

agent (CTA) for a chain extension of PNIPAAm-*st*-PTlAm second block. PTlAm units were ring opened by alkyl amines to form thiol groups, which were subsequently reacted with the acrylamide-coated MNP to obtain the copolymer-coated particle. PDEAEMA block was then quaternized to obtain cationic MNP to improve the water dispersibility of the particle and for ionic adsorption with negative bio-entities. The effect of alkyl chain lengths (C3, C8 and C12) on the assemblies of the copolymer-coated MNP, affecting their water dispersibility and magnetic separation ability, was investigated. Moreover, the temperature change and the effect of alkyl chain lengths on the rate of the drug release (doxorubicin as a model drug) was also studied (Figure 1.1).

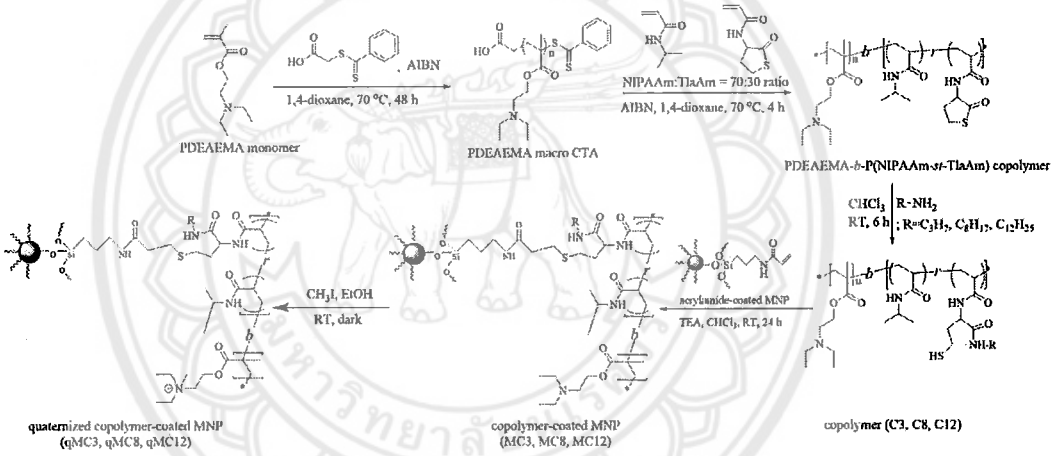

Figure 1.1 Synthetic scheme of the copolymer-coated MNP (MC) and its quaternization (qMC)

Research objectives

This work focuses on the surface modification of MNP with PDEAEMA-*b*-P(NIPAAm-*st*-TlaAm) copolymer to obtain magnetic nanocluster with bilayer copolymer coating with thermo-responsive properties for drug controlled release application. The effect of temperature changes on drug releasing behavior of the copolymer-coated MNP will be demonstrated.

Research scopes

1. Design and synthesis of thermo-responsive PDEAEMA-*b*-P(NIPAAm-*st*-TlaAm)

2. Immobilization of the synthesized copolymer on MNP surface

3. Study in the effect of temperature change on drug releasing behavior of the copolymer bilayer-coated MNP

CHAPTER II

LITERATURE REVIEW

This research focused on the synthesis of thermo-responsive functional diblock copolymer containing TlaAm moiety for coating on MNP surface and obtain amphiphilic copolymer bilayer for controlled and sustained release of the entrapped drug. This copolymer was synthesized *via* RAFT polymerization using a PDEAEMA macro chain transfer agent (CTA) to mediate the polymerization of statistical P(NIPAAm-*st*-TlaAm) block (Figure 2.1). The TlaAm units were ring-opened with primary alkylamine to form thiol groups (-SH), followed by the thiol-ene coupling reactions with acrylamide-grafted MNP. 1-propylamine, 1-octylamine and 1-dodecylamine were used in the ring-opening reactions to investigate the effect of degree of hydrophobicity due to various chain lengths of alkyl groups on the aggregation, water dispersibility and morphology of the copolymer-coated MNP. PDEAEMA block in the copolymer was subsequently quaternized with CH_3I to give good water dispersibility to the copolymer-grafted MNP. This novel polymer-MNP hybrid was well designed to be used in drug controlled release application.

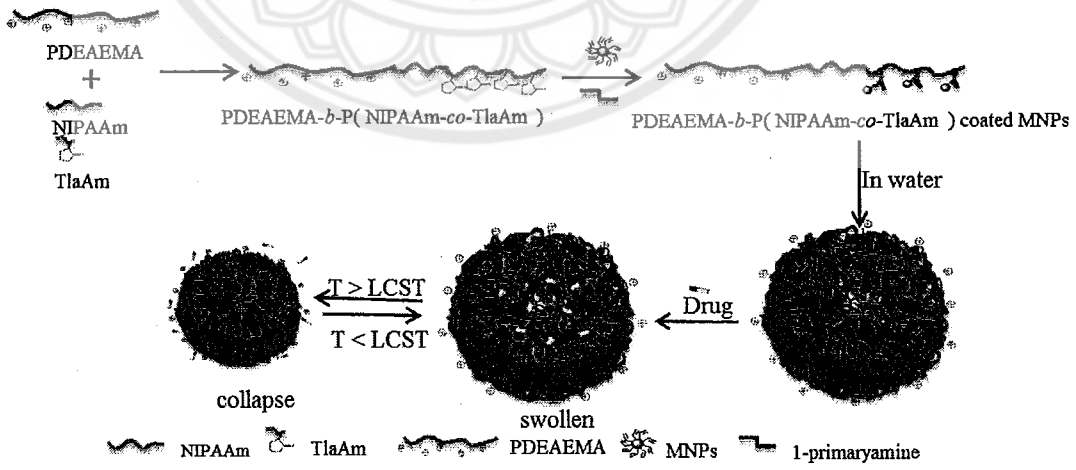

Figure 2.1 Synthesis of the copolymer-coated MNP to form polymeric bilayer for use in drug controlled release application

Because the experimental section in this project was divided into 3 parts: 1) synthesis of PDEAEMA-*b*-P(NIPAAm-*st*-TlaAm) copolymer, 2) modification of the synthesized copolymer on MNP surface and 3) study in the effect of temperature change on drug releasing behavior of the copolymer-coated MNP, therefore, the literature reviews are divided into 3 parts as following;

1. thermo-responsive polymers
2. poly(*N*-thiolactone acrylamide) (PTlaAm)
3. polymer-coated MNP

1. Thermo-responsive polymers

There are two main types of thermo-responsive polymers; the first contains a lower critical solution temperature (LCST) and the second has an upper critical solution temperature (UCST). LCST is the critical temperature point below which the polymer and solvent are completely miscible as shown in Figure 2.2 [39]. Similarly, in the case of UCST, the polymer and solvent are miscible at above UCST critical temperature point. Therefore, at temperature below LCST, a polymer solution appears clear and homogenous, but a polymer solution will turn cloudy at temperature above LCST. Therefore, LCST is also referred to as the minimum of the cloud point curve on temperature-polymer volume fraction (ø) phase diagram. The variable appearances of polymer solution at different temperatures depend on whether the interaction of polymer and solvent are energetically favorable. In particular, considering the free energy of the system using the Gibbs equation:

$$\Delta G = \Delta H - T\Delta S$$

where ΔG is Gibbs free energy, ΔH is enthalpy and ΔS is entropy.

Increase in temperature augments the entropy of the system causing the phase separation to be more favorable. Entropy of the water plays a major role in the determination of polymer solubility because the presence of polymer in a solution causes the water molecules to be less ordered and have higher entropy. This is also

called the "hydrophobic effect" [40-42]. It is known that LCST provides an entropically driven effect while UCST is an enthalpically driven effect [43].

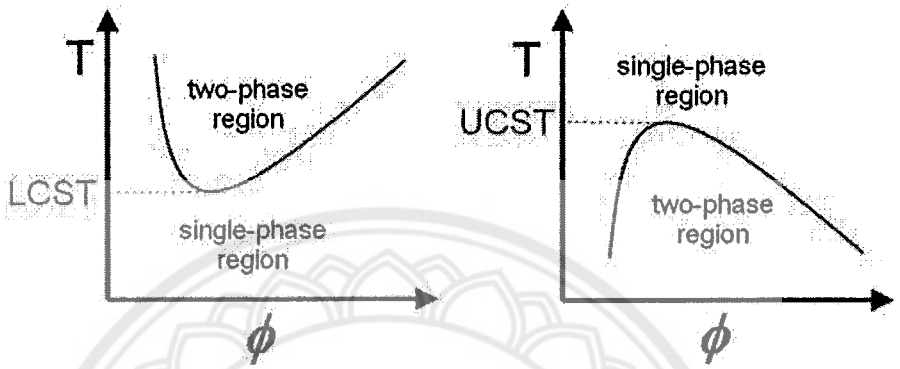

Figure 2.2 A temperature (T) *vs.* polymer volume fraction (ø) plot. Schematic illustration of phase diagrams for polymer solution (a) LCST behavior and (b) UCST behavior [39]

Most of the studies detailed in this review use polymers that have an LCST. PNIPAAm, polymerized from NIPAAm monomer (Figure 2.3), is one of the best known and most studied thermo-responsive polymers in this class. PNIPAAm exhibits phase separation at a certain temperature, which is referred to as LCST. PNIPAAm has a LCST of about 32 °C in aqueous solution [44-48]. When the temperature is below its LCST, PNIPAAm is hydrophilic and soluble in water (Figure 2.4). The polymer chains are well hydrated and completely extended with intermolecular hydrogen bonding between the water molecules and the polymer chains (Figure 2.5). On the other hand, at a temperature above its LCST, the chains abruptly collapse resulting in an increase in hydrophobicity and exclusion of water, resulting in the formation of intermolecular hydrogen bonding among the polymer chains.

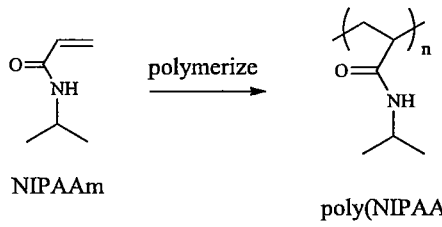

Figure 2.3 Chemical structure of *N*-isopropylacrylamide (NIPAAm) and PNIPAAm

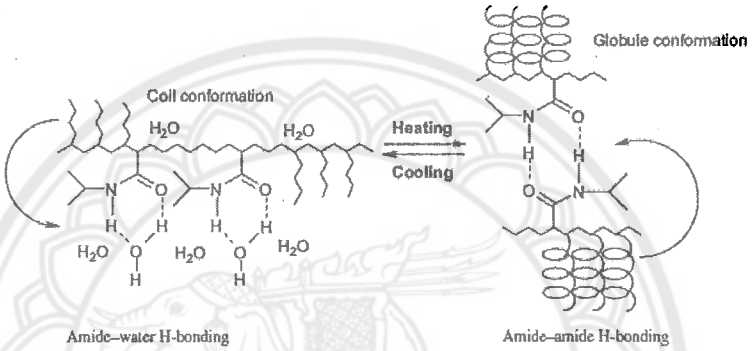

Figure 2.4 H-bonding between amide-water (hydration) and amide–amide (dehydration) giving a potential role in its phase transition behavior [49]

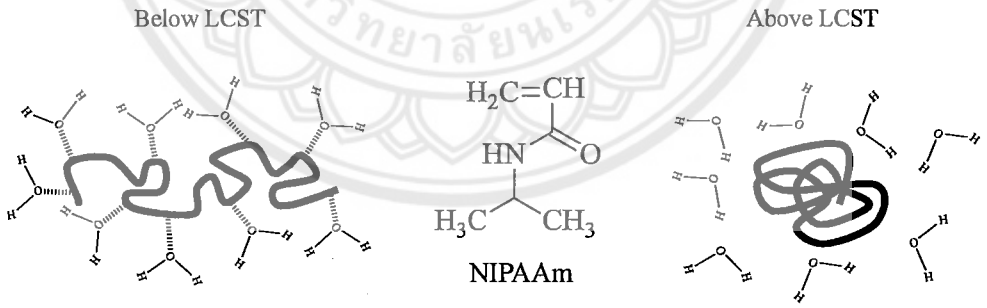

Figure 2.5 H-bonding between PNIPAAm chains and water molecules as a function aof temperature at above and below LCST [49]

Zhou, *et al.* have presented RAFT polymerization and dually responsive behaviors of terpyridine-containing PNIPAAm copolymers in dilute solutions (Figure 2.6) [50]. They showed the development of terpyridine-containing PNIPAAm copolymers to obtain the copolymers that gave the properties of thermo-responsive

polymers and sensitive metal ion. The molecular structures of the polymers had been confirmed by fourier transform infrared spectroscopy (FTIR), proton nuclear magnetic resonance spectroscopy (^{1}H NMR). From the transmittance of the polymer solution, the LCST of poly(NIPAAm-*co*-TpyPhA) was 28 ^{o}C, while the responsiveness to Fe^{2+} was fast from colorless state into purple state due to the coordination between Fe^{2+} and terpyridine in poly(NIPAAm-*co*-TpyPhA) chain (Figure 2.7). This information provided some clues for developing new multi-responsive and multi-functional polymers.

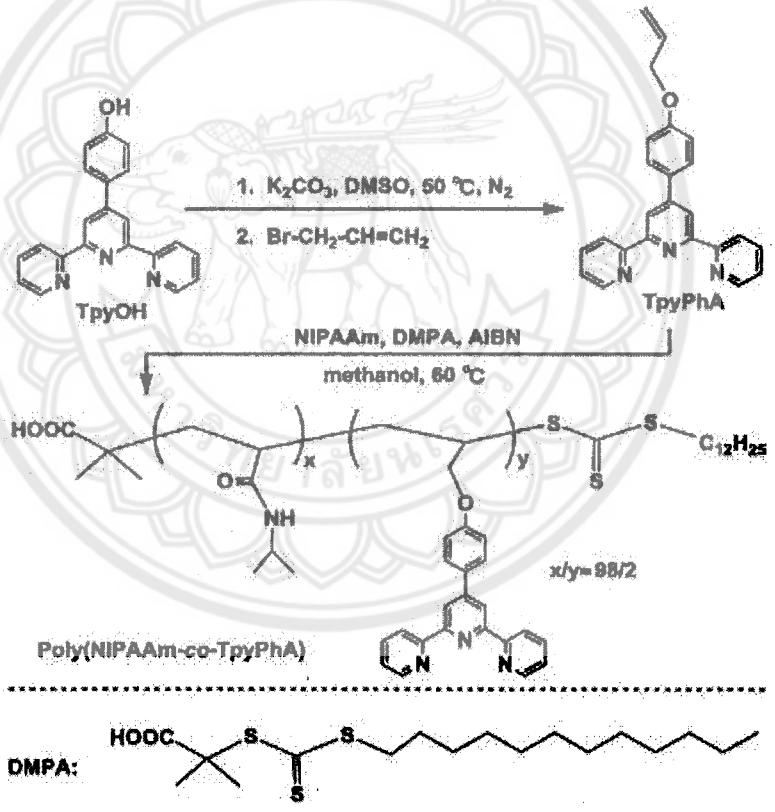

Figure 2.6 Schematic illustration of the synthetic route for poly(NIPAAm-co-TpyPhA) [50]

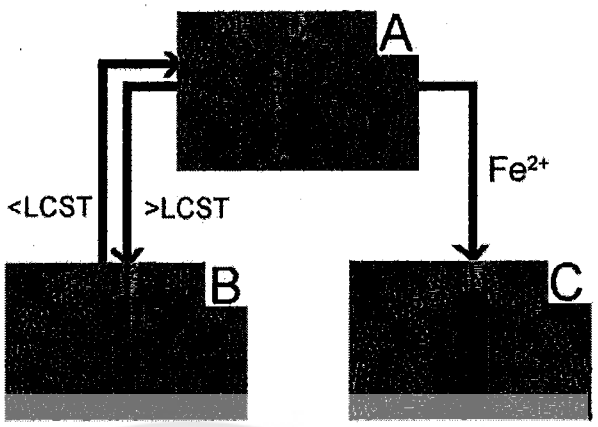

Figure 2.7 The thermo-responsive polymers and sensitive metal ion of poly(NIPAAm-co-TpyPhA) [50]

Barnes, *et al.* have presented the synthesis of collagen-PNIPAAm hydrogels with tunable properties (Figure 2.8) [51]. A combining collagen with a poly(NIPAAm-*co*-styrene-*graft*-NVP) (NSN) was developed to improve mechanical properties and to maintain cytocompatibility. It was found that the resulting hydrogel syneresis, mechanical properties and cytocompatibility can be tuned by adjusting the ratio of collagen to NSN. They found that more than 2.5 wt% collagen combined NSN were able to form self-supporting gels; they were suitable for use as cell scaffolds.

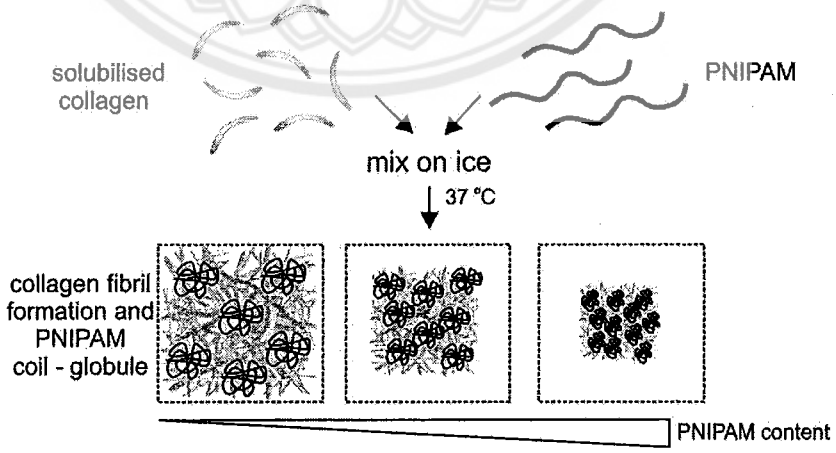

Figure 2.8 Schematic illustration the collagen-PNIPAAm hydrogels [51]

In 2011, Fan, *et al.* have demonstrated the synthesis of a novel thermo and pH responsive magnetic hydrogel nanosphere of poly(*N*-isopropylacrylamide-*co*-acrylic acid)/MNPs (P(NIPAAm-*co*-AA)/MNPs) for drug release application [52]. The procedure to prepare poly(NIPAAm-*co*-AA)/MNPs hydrogel nanospheres composed of three steps (Figure 2.9). A stable dispersion of MNPs modified by citrate groups was first dispersed in NIPAAm and AA solutions, which then polymerized by using potassium persulfate (KPS) as an initiator and *N,N*-methylenebis(acrylamide) (BIS) as a crosslinker, resulting in the formation of the P(NIPAAm-*co*-AA) polymer magnetic hydrogel nanospheres. These nanospheres were analyzed particle sizes and shapes by TEM technique. It was found that the magnetic hydrogel nanospheres had uniform sphere structures and the average diameter of such a structure was 150 nm.

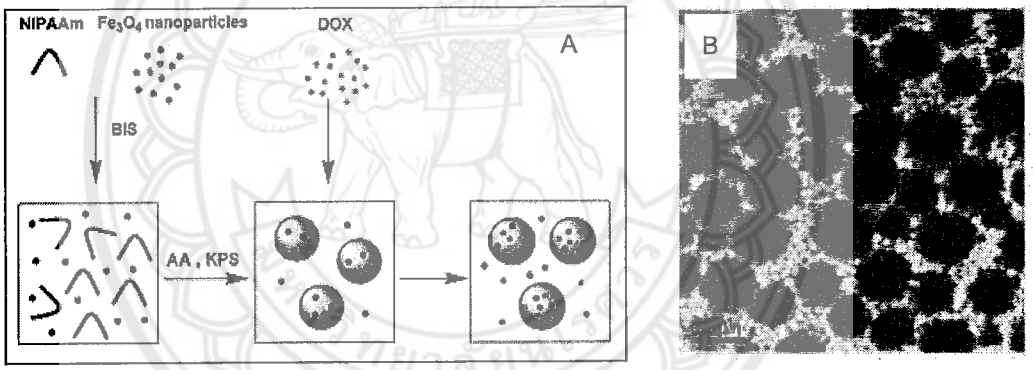

Figure 2.9 Preparation (A) and TEM micrographs (B) of the drug-loaded P(NIPAAm-*co*-AA)/MNP hydrogel nanospheres [52]

2. Poly(*N*-thiolactone acrylamide) (PTlaAm)

Thiolactone monomer can be synthesized via the nucleophilic substitution between D,L-homocysteine thiolactone and acryloyl chloride (Figure 2.10).

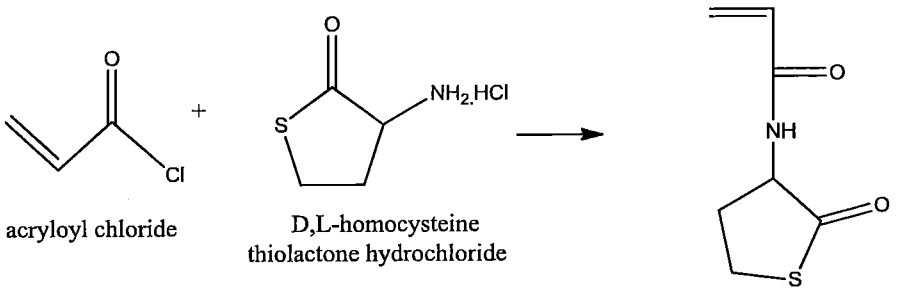

acryloyl chloride D,L-homocysteine thiolactone hydrochloride thiolactone monomer

Figure 2.10 Synthesis and chemical structure of a thiolactone monomer

Chain polymerization of thiolactone monomer to obtain polythiolactone (PTlaAm) is shown in Figure 2.11.

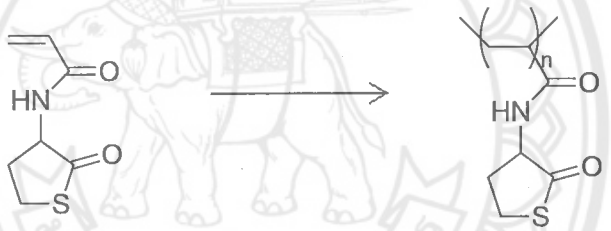

Figure 2.11 Chain polymerization of thiolactone monomer to obtain polythiolactone (PTlaAm)

This polymerization reaction gives good electrophilic PTlaAm with no by-product after the ring-opening reaction. The formation of thiol (-SH) allows for the second modification after the ring-opening reaction. Belbekhouche, *et al.* have presented the polythiolactone-based redox responsive layers for the reversible release of functional molecules (Figure 2.12) [53]. A novel copolymer of the TlaAm and *N,N*-dimethylacrylamide (DMA) was synthesized via RAFT polymerization. After the ring opening reaction of the polythiolactones with amine derivatives and essentially form free thiol groups, they were successfully grafted onto flat gold surfaces. The presence of polythiol layers on gold substrates were confirmed *via* various techniques such as electrochemical Impedance spectroscopy, water contact

angle measurement, X-ray photoelectron spectroscopy, and X-ray reflectometry. These layers were functionalized with rhodamine B-poly(ethylene glycol)-thiol, a thiolated dye, which could be released in reducing conditions and again re-grafted in oxidizing conditions.

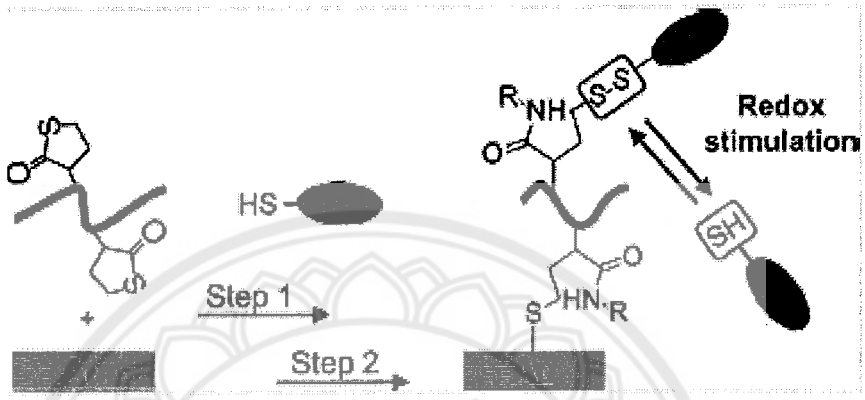

Figure 2.12 The design of polythiolactone-based redox responsive layers on gold surface [53]

Reinicke, *et al.* reported a quantitative, additive-free, and one-pot reaction involving the ring-opening reaction of poly(N-isopropyl acrylamide-co-N-thiolactone acrylamide) (poly(NIPAAm-co-TlaAm)) by primary amine treatment and subsequent conversion of the released thiol groups *via* a Michael addition reaction with acrylate functional groups [54]. This was used for the double modification/functionalization of the polyNIPAAm-containing polymers, yielding tailor-made thermo-responsive polymers. It was found that the cloud points of the polymer-containing solutions can be tuned by adjusting the amount of loaded amines in the ring-opening reactions, allowing for the control of the degree of the modification (Figure 2.13).

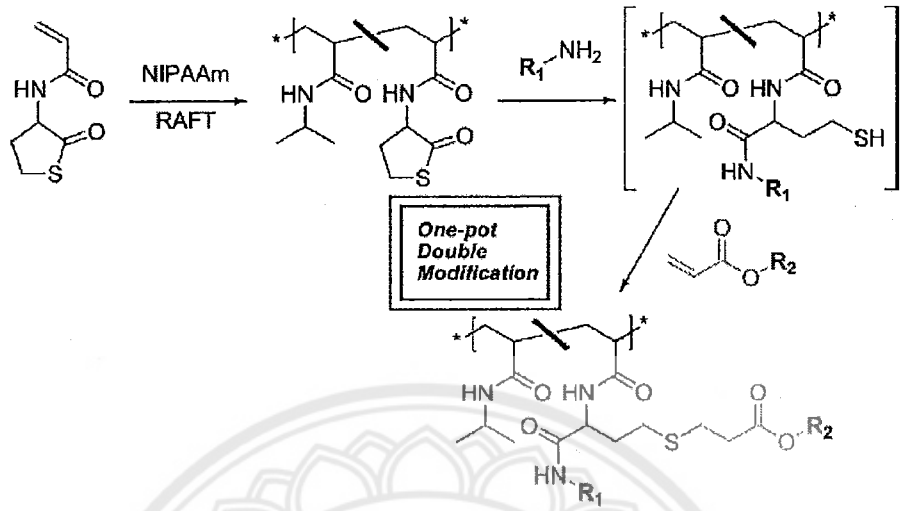

Figure 2.13 One-pot double modification of p(NIPAAm-co-TlaAm) [54]

Chen and co-workers recently reported the synthesis of the copolymer of TlaAm and NIPAAm *via* RAFT polymerization [55]. This copolymer was then reacted with various 1-amino alkyl compounds to obtain thiol groups after the ring-opening reaction, and followed by the coupling of the thiol groups (-SH) with sugar derivatives to obtain the double-modified graft copolymers (Figure 2.14). They were able to self-assemble as micellar structure due to their amphiphilic nature. The sizes of the micelles increased from 200 to 600 nm in diameter when the loaded alkyl amines were increased, and the assembled nanoparticles were bioactive and can interact effectively with Concanavalin A (ConA) lectin.

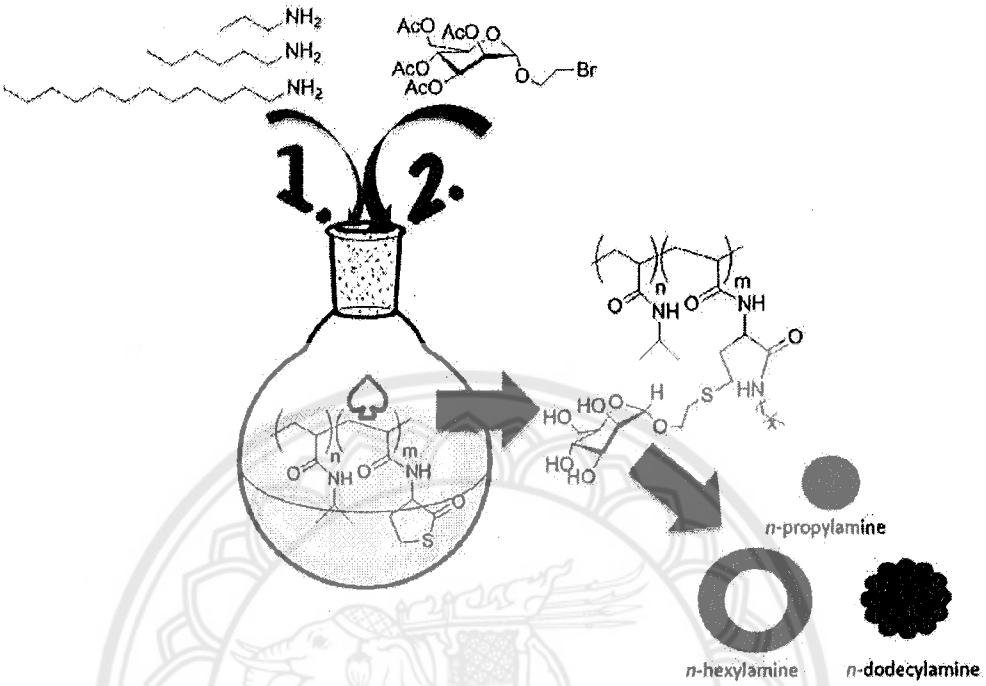

Figure 2.14 One-pot reactions of glycopolymer-based nanoparticles, employing a double modification (aminolysis and nucleophilic substitution) of thiolactone-containing polyacryl-amides [55]

3. Polymer-coated MNP

Because MNP is in nano-scale that has a high surface area-to-volume ratio, it is not stable, leading to aggregation in dispersions due to attractive forces among the particles. Large clusters of aggregates take place during or after the synthesis of the MNP because of these attractive forces in order to minimize the total surface energy. Therefore, stabilization of MNP by surface modification is necessary to protect them from particle aggregation.

Sahoo, *et al.* have presented the synthesis of thermal and pH responsive polymer-tethered multifunctional magnetite nanoparticles (MNP) for targeted delivery of anticancer drug (Figure 2.15) [1]. Amino-grafted MNP surface by co-precipitation were covalently coupling with -COOH of PNIPAAm-*b*-polyacrylic acid (PAA) copolymers. Then, the surface was modified with folic acid (FA) and rhodamine B

isothiocyanate (RITC), followed by loading of doxorubicin (DOX) into the particle surface. The magnetic core and polymer shell structure of the particles prepared was confirmed by X-ray diffraction (XRD) and FTIR spectroscopy. The release of the DOX-loaded MNP was studied by fluorescence microscopy about 25 and 37 °C. It was found that the release amount and rate depend on pH and temperature.

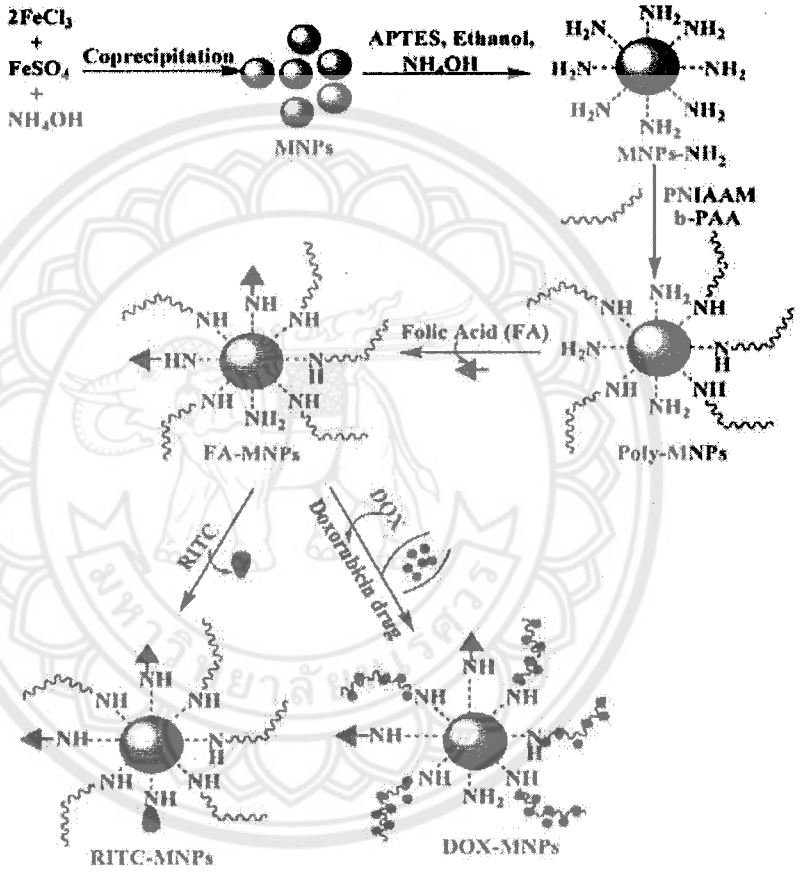

Figure 2.15 The designing of thermal and pH responsive polymer-tethered multifunctional magnetite nanoparticles (MNP) [1]

Meerod, *et al.* have presented the modification of hydrophilic poly(NIPAAM-*co*- poly(ethylene glycol) methacrylate)-coated MNP nanoclusters with thermo-responsive properties and their drug controlled release (Figure 2.16) [32]. These magnetic nanoclusters were synthesized via an *in situ* radical polymerization in the presence of acrylamide-grafted MNP. PNIPAAm provided thermo-responsive

properties, while poly(ethylene glycol) methacrylate (PEGMA) provided good water dispersibility; the nanoclusters were well dispersible in water at room temperature and can be agglomerated when temperature above the LCST (32 °C). The release behavior of an indomethacin model drug from the nanoclusters was investigated during stepwise temperature between 15 °C and 45 °C. It was found that the ratio of PEGMA to NIPAAm in the MNP nanoclustering influenced the entrapment efficiency as well as the release behavior of an indomethancin model drug.

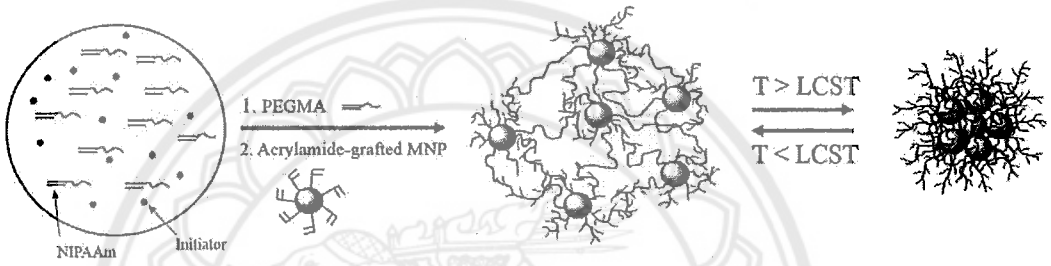

Figure 2.16 The formation of the thermo-responsive poly(NIPAAM-*co*-PEGMA)-grafted MNP nanoclusters [32]

Chen, *et al.* have presented the synthesis of thermo-responsive hollow magnetic microspheres with hyperthermia and controlled release properties (Figure 2.17) [7]. A carbon nanomaterial was used as a steric stabilizer for MNP and a supporter for PNIPAAm. Thermo-responsive NIPAAm was grafted on the carbon-encapsulate hollows by surface radical polymerization. The thermo-responsive hollow magnetic microspheres were confirmed by XRD, SEM and TEM measurements. The results showed that the microspheres had a phase-transition temperature around 43 °C and a saturation magnetization of 56.9 emu/g. The 5-fluorouracil model drug was loaded in and released from the microspheres with different release rates at 35 and 50 °C.

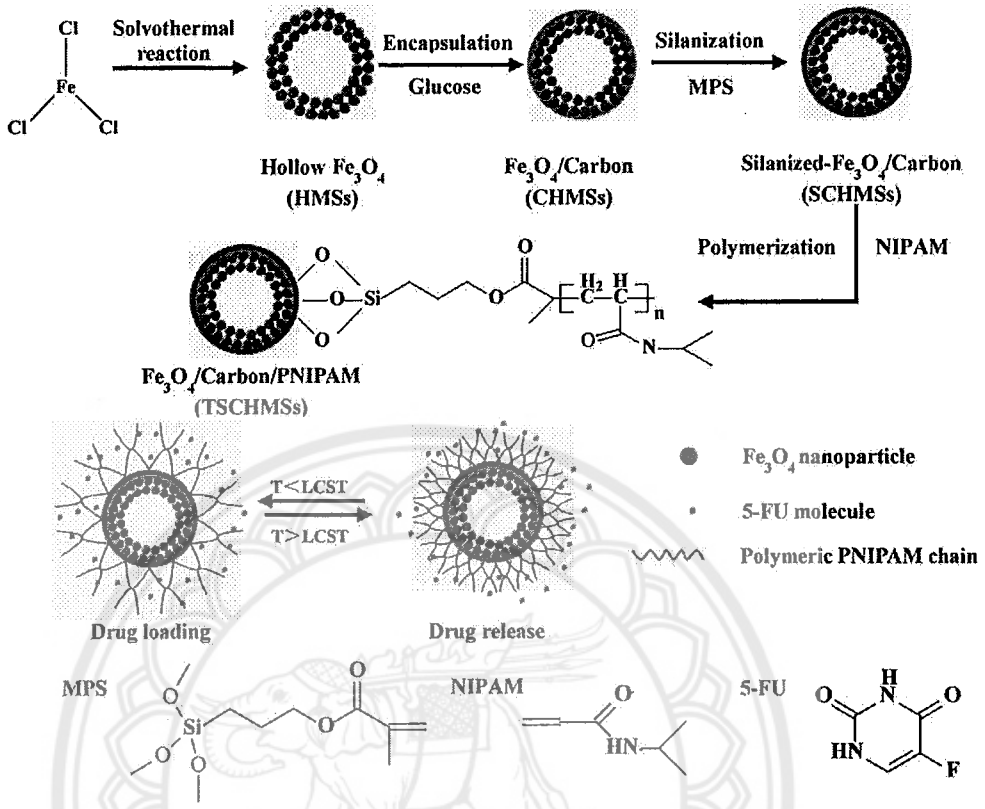

Figure 2.17 Synthesis, drug loading, and release of the thermo-responsive hollow magnetic microspheres [7]

Wan, *et al.* have prepared stable MNP in aqueous dispersions by coprecipitation of aqueous ferrous (Fe^{2+}) and ferric (Fe^{3+}) solutions in a base in the presence of poly(glycerol monoacrylate)-*g*-poly(PEG methyl ether acrylate) (PGA-*g*-PEG) graft copolymers (Figure 2.18) [56]. PGA-*g*-PEG was prepared by acidic hydrolysis of poly(solktal acrylate)-*g*-poly(PEG methyl ether acrylate), which was synthesized by copolymerization of solktal acrylate and PEG methyl ether acrylate by atom transfer radical polymerization (ATRP). The size of the copolymer-stabilized MNP can be controlled from 4 nm to 18 nm by varying the graft density of the graft copolymers.

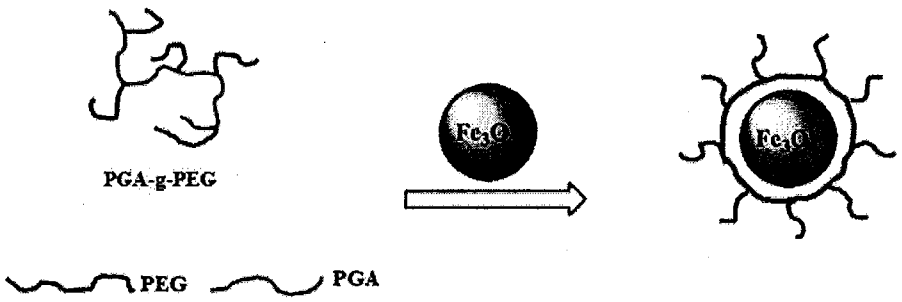

Figure 2.18 Stabilization of MNP with PGA-*g*-PEG copolymer [56]

Fan, *et al.* have reported the grafting reaction of poly(ethyleneglycol) monomethacrylate (PEGMA) on MNP surface *via* a solvent-free atom transfer radical polymerization (ATRP) (Figure 2.19) [57]. MNP was prepared *via* a high-temperature decomposition of $Fe(acac)_3$. The macroinitiators were immobilized on the surface of 6.5±0.8 nm MNP *via* effective ligand exchange of oleic acid with 3-chloropropionic acid (CPA). The surface-modified MNP was well dispersible in the PEGMA monomer. The ligand exchange method enabled dispersibility of the MNP to fulfill the requirement of solvent-free ATRP since CPA, the surface capping agents, can be exchanged in a controllable fashion, depending on the functional groups and concentrations of the surfactants. The PEGMA-grafted MNP has a uniform hydrodynamic particle size of 36.0±1.2 nm. The physical properties, cytotoxicity and MRI of the PEGMA-grafted MNP were investigated and the results showed that these MNP may be a good candidate for bio-applications.

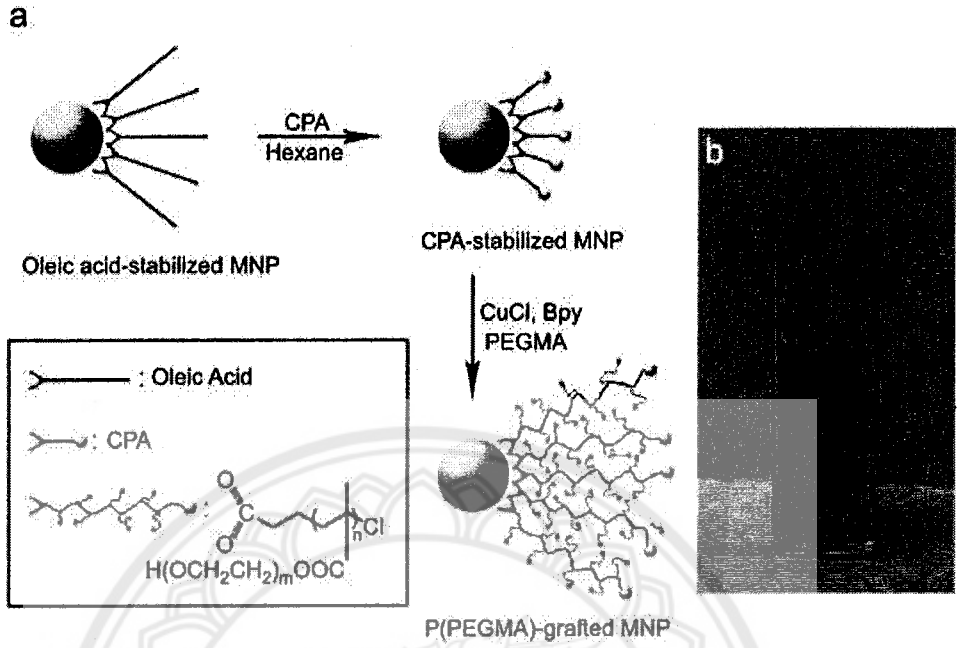

Figure 2.19 Preparation route of (a) P(PEGMA)-grafted MNP by solvent-free ATRP and (b) a photograph of PEGMA-grafted MNP dispersion in water [57]

Galeotti, et al. have reported a detailed study of surface modification of MNP by means of three different grafting organosilane agents for preparation of magnetic polymer brushes (Figure 2.20) [58]. 3-Aminopropyltriethoxysilane (APTES), 3-chloropropyl-triethoxysilane (CPTES) and 2-(4-chlorosulfonylphenyl) ethyltrichlorosilane (CTCS) were selected as grafting models through which a wide range of polymer brushes can be obtained. By means of accurate thermogravimetric analysis, it was found that a good control over the amount of immobilized molecules was achieved, and optimal operating conditions for each grafting agent were consequently determined. Graft densities ranging from 4 to 7 molecules per nm^2 were obtained depending on the conditions used. In addition, the surface-initiated ATRP of methyl methacrylate (MMA) carried out with CTCS-coated nanoparticles was presented as an example of polymer brushes, leading to a well-defined and dense polymeric coating of around 0.6 poly(methyl methacrylate) (PMMA) chains per nm^2.

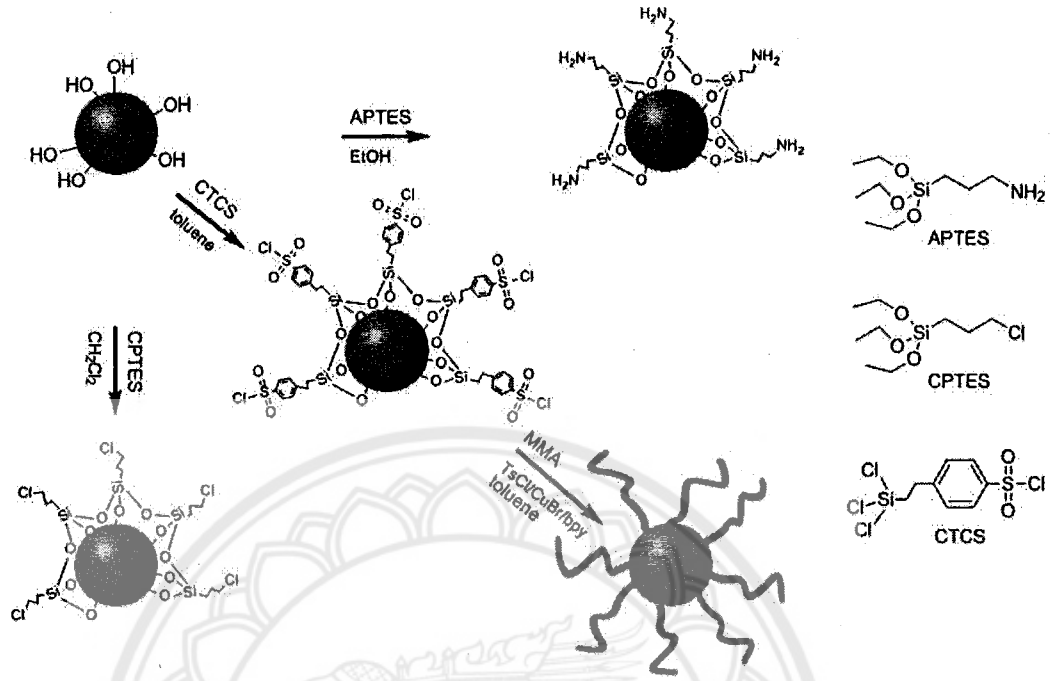

Figure 2.20 Reaction scheme and organosilane structures employed for the functionalization of MNP surface [58]

Rutnakornpituk, et al. have prepared poly(acrylic acid) (PAA)-grafted MNP *via* surface-initiated ATRP of *t*-butyl acrylate, followed by acid-catalyzed deprotection of *t*-butyl groups (Figure 2.21) [59]. In addition to serve as both steric and electrostatic stabilizers, PAA grafted on MNP surface also served as a platform for conjugating folic acid, a cancer cell targeting agent. The particle size was 8 nm in diameter without significant aggregation during the preparation process. This novel nanocomplex is hypothetically viable to efficiently graft other affinity molecules on their surfaces and thus might be suitable for use as an efficient drug delivery vehicle particularly for cancer treatment.

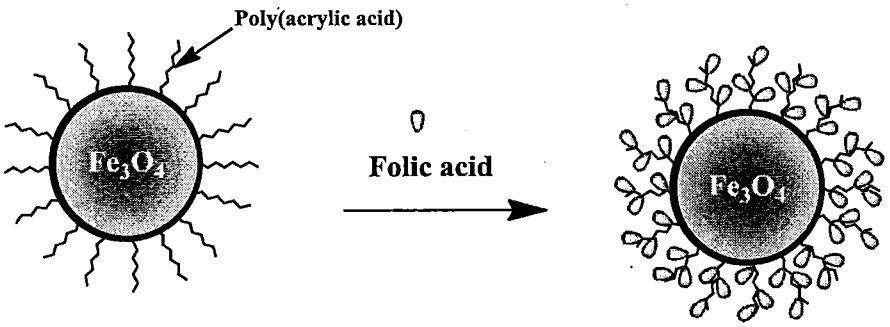

Figure 2.21 Immobilization of folic acid on the surface of PAA-coated MNP [59]

CHAPTER III

RESEARCH METHODOLOGY

The aim of this work is to modify surface of MNP with PDEAEMA-*b*-P(NIPAAm-*st*-TlaAm) copolymer to obtain magnetic nanocluster with bilayer copolymer coating with thermo-responsive properties for drug controlled release application. In addition, the effect of temperature changes on drug releasing behavior of the copolymer-coated MNP will be studied.

Materials

Unless otherwise stated, the reagents were used without purification: iron(III) acetylacetonate ($Fe(acac)_3$, 99%, Acros), aminopropyltriethoxysilane (APTES, 99%, Acros), *D,L*-homocysteine thiolactone hydrochloride (99%, Acros), oleic acid (Carlo Erba), (3-aminopropyl) triethoxysilane (APTES, 99%, Acros), triethylamine (TEA, 97%, Carlo Erba), 2,2'-azobis(2-methylpropionitrile) (AIBN, 98%, Sigma-Aldrich), s-(thiobenzoyl) thioglycolic acid as a chain transfer agent (99%, Aldrich), 2-(diethylamino) ethyl methacrylate (DEAEMA, 99% stabilized, Acros), and *N*-isopropylacrylamide (NIPAAm, 99%, Acros) were used as received. Acryloyl chloride was synthesized prior to use *via* a chloride exchange reaction between acrylic acid (98%, Acros) and benzoyl chloride (99%, Acros) to obtain a colorless liquid with 60% yield. 1-Propylamine (99%, Sigma-Aldrich), 1-octylamine (99%, Merck), 1-dodecylamine (98%, Acros) and iodomethane (2.0 M in tert-butyl methyl ether, Sigma-Aldrich) were used as received. Doxorubicin hydrochloride (DOX, 2 mg/ml, Pharmachemie BV) were used as received.

Syntheses

Synthesis of N-thiolactone acrylamide (TlaAm) monomer

To the mixture of *D,L*-homocysteine thiolactone hydrochloride (7.05 g, 45.6 mmol) in a H_2O/1,4-dioxane solution (100 ml), $NaHCO_3$ (19.20 g, 227.9 mmol) was added and stirred for 30 min in an ice bath. Acryloyl chloride (8.3 g, 91.2 mmol) was then added dropwise and stirred at room temperature overnight. After the reaction completed, brine (100 ml) was added into the solution, followed by extracting with ethyl acetate (3×200 ml) to obtain TlaAm in an organic layer. Finally, TlaAm monomer was purified by recrystallization from CH_2Cl_2 and then dried *in vacuo*.

Synthesis of acrylamide-coated MNP

MNP was synthesized *via* a thermal decomposition method of $Fe(acac)_3$ (5 g, 14.1 mmol) in 90 ml benzyl alcohol at 180 °C for 48 h. Then, the particle was magnetically separated and washed with ethanol and then chloroform. Oleic acid (4 ml) was slowly added to the MNP-toluene dispersion (30 ml) with sonication to form oleic acid-coated MNP, followed by an addition of APTES (4 ml) containing TEA (2 ml) to form amino-coated MNP. After stirring for 24 h, the particles were precipitated in ethanol and washed with toluene. After re-dispersing the particles (0.1 g) in a NaOH solution (6.72 mmol in 10 ml DI), acryloyl chloride (3.36 g, 37.1 mmol) was then added to the dispersion and stirred for 24 h. The product was magnetically separated, repeatedly washed with water and then stored in the form of dispersions in THF (0.1 g MNP/1 ml).

Synthesis of PDEAEMA macro chain transfer agent (PDEAEMA macro CTA)

DEAEMA monomer (1.9361 g, 10.4 mmol), S-(thiobenzoyl) thioglycolic acid (31.7 mg, 0.1 mmol) as CTA and AIBN initiator (4.9 mg, 0.03 mmol) ($[DEAEMA]_0$:[CTA]:[AIBN] molar ratio of 70:1:0.2, respectively) were dissolved in 1,4-

dioxane (7 ml) under N_2 atmosphere with stirring for 30 min. The RAFT polymerization was performed for 48 h at 70 °C to obtain *ca*.50% monomer conversion with $\overline{M_n}$ of PDEAEMA about 6,700 g/mol (Supplementary material Figure S1). The polymerization was ceased by cooling at room temperature in air. The PDEAEMA macro CTA was purified by dialysis in methanol and dried *in vacuo*.

Synthesis of PDEAEMA-b-P(NIPAAm-st-TlaAm) block copolymer

PDEAEMA macro CTA (0.06 mmol), NIPAAm (4.24 mmol), TlaAm (1.82 mmol) and AIBN initiator (0.01 mmol) ($[NIPAAm]_0$:$[TlaAm]_0$:[PDEAEMA macro CTA]:[AIBN] molar ratio of 70:30:1:0.2, respectively) was dissolved in 1,4-dioxane (8.5 ml) under N_2 atmosphere with stirring for 30 min. The RAFT polymerization was performed at 70 °C for 4 h to obtain *ca*.50% NIPAAm conversion and 30% TlaAm conversion with $\overline{M_n}$ of the copolymer about 12,200 g/mol (Supplementary material Figure S2). The polymerization was stopped by cooling at room temperature with air. The copolymer was purified by dialysis in methanol and dried *in vacuo*.

Synthesis of the copolymer-coated MNP by a double modification of PDEAEMA-b-P(NIPAAm-st-TlaAm) copolymer

The copolymer (0.16 mmol of TlaAm unit) was dissolved in chloroform (5 ml) followed by an addition of primary alkylamines (0.32 mmol, 2:1 molar ratio of alkyl amine to TlaAm unit), e.g. 1-propylamine, 1-octylamine and 1-dodecylamine, to obtain the C3, C8 and C12 copolymers, respectively. The solution was then mixed with the acrylamide-coated MNP (100 mg) and TEA (0.1 ml) and stirred for 24 h under N_2 gas. The copolymer-coated MNP was magnetically separated and washed with chloroform and designated as MC3, MC8 and MC12, respectively.

Quaternization of PDEAEMA in the copolymer-coated MNP

The copolymer-coated MNP (1.76 mmol of DEAEMA units) was re-dispersed in ethanol (40 ml), followed by dropwise addition of 2M CH_3I solution (1.76 mmol). The mixture was stirred for 20 h in dark at room temperature. The quaternized products (qMC3, qMC8 and qMC12) were magnetically separated and washed with THF to remove an excess of CH_3I, followed by drying *in vacuo* to obtain black powder.

In vitro release studies of entrapped DOX from the copolymer-coated MNP

The drug solution (2 mg/ml of DOX) was added dropwise into the quaternized MNP dispersions (10 mg/2 ml in DI water) with stirring at 15 °C for 3 h. The DOX-entrapped MNP was separated from an excess DOX by magnetic separation for 30 min and washed with DI water for 4 times. The dispersion of DOX-entrapped MNP (10 mg in 3 mL DI water) was placed in a water bath at 25 °C (below LCST of PNIPAAm) for 1 h and then temperature was increased to 45 °C (above LCST of PNIPAAm) for another 80 min. During the experiment, 0.2 ml of the dispersions was withdrawn from the release media at a pre-determined time until the released drug reached the equilibrium (the total time points ranging between 12 and 15). After 30-min magnetic separation, the concentrations of the released drug in the supernatant at a given time were determined *via* UV-visible spectrophotometry at λ= 480 nm and % drug release was calculated from the following equation;

$$\%\ \text{drug released} = \frac{\text{Weight of released drug at a given time}}{\text{Weight of the entrapped drug in the MNP}} \times 100$$

where the weight of the entrapped drug in the MNP was determined from the amount of the drug at the maximum point of the release profile combined with those remaining in the particles. To dissolve the remaining drug from the MNP, DI water (3 ml) was added to the particles and then the mixture was heated at 50 °C for 1 h. After 30-min magnetic separation, the drug concentration in the supernatant was

then determined *via* UV-visible spectrophotometry. The drug entrapment efficiency was calculated from the following equation;

$$\textbf{Entrapment efficiency (\%EE)} = \frac{\textbf{weight of the entrapped drug in the MNP}}{\textbf{weight of the loaded drug}} \textbf{ x 100}$$

Characterization

FTIR spectrophotometry was operated on a Perkin–Elmer Model 1600 Series FTIR spectrophotometer. ^{1}H NMR spectroscopy was performed on a 400 MHz Bruker NMR spectrometer using DMSO-d_6 or $CDCl_3$ as solvents. The hydrodynamic diameter (D_h) and zeta potential of the particles were measured by PCS using NanoZS4700 nanoseries Malvern instrument. The sample dispersions were sonicated for 1 h before each measurement without filtration. The TEM images were conducted using a Philips Tecnai 12 operated at 120 kV equipped with Gatan model 782 CCD camera. The particles were re-dispersed in water and then sonicated before deposition on a TEM grid. TGA was performed on Mettler-Toledo's SDTA 851 at the temperature ranging between 50 and 800 °C and a heating rate of 20 °C/min under oxygen atmosphere. Magnetic properties of the particles were measured at room temperature using a Standard 7403 Series, Lakeshore vibrating sample magnetometer (VSM). UV-visible spectrophotometry was performed on microplate reader at λ = 480 nm.

CHAPTER IV
RESULTS AND DISCUSSION

This work focused on the surface modification of MNP with multi-functional PDEAEMA-*b*-P(NIPAAm-*st*-TlaAm) copolymer to obtain magnetic nanocluster with thermo-responsive properties for drug controlled release application. The copolymer was synthesized *via* RAFT polymerization to control architecture and the molecular weight of the block copolymer. PDEAEMA macro CTA was first synthesized, followed by the extension of P(NIPAAm-*st*-TlaAm) second block from PDEAEMA first block. It was envisioned that the quaternized PDEAEMA could form the corona, while P(NIPAAm-*st*-TlaAm) block self-assembled to be a core in aqueous media. (Supplementary material Figure S3). PTlaAm in the P(NIPAAm-*st*-TlaAm) allowed for a double modification for 1) adjustment of the degree of the hydrophobicity of the polymeric core and 2) immobilization of the polymer on MNP surface. This P(NIPAAm-*st*-TlaAm) core was also used for entrapment of a therapeutic drug with a thermo-triggering release mechanism owing to the existence of PNIPAAm in the structure. In addition, an optimal degree of hydrophilicity/hydrophobicity of the copolymer might be necessary for controlled release of the entrapped drug. Therefore, three different alkyl chain lengths (C3, C8 and C12) were used for tuning the degree of the hydrophobicity of the copolymer coated on the particle surface.

Synthesis and characterization of the copolymer-coated MNP

^{1}H NMR spectra of the purified products from each step were shown in Figure 4.1. The signals corresponding to the methylene protons of PDEAEMA macro CTA (1.8-1.9 ppm) indicated the polymerization of PDEAEMA (Figure 4.1A). This macro CTA was then used for the propagation of NIPAAm and TlaAm monomers. The new signals at δ 1.1 and 3.6 ppm of the NIPAAm units and at δ 3.2 and 4.7 ppm of TlaAm units indicated the propagation of both monomers from PDEAEMA macro CTA (Figure 4.1B).

After the ring-opening reactions of thiolactone units with various alkylamines (1-propylamine, 1-octylamine and 1-dodecylamine), the strong signals of the protons of alkyl groups appeared in the range of δ 0.9- 1.4 ppm (Figure 4.1C, 4.1D, and 4.1E). In good agreement with this result, the disappearance of TlaAm signals at δ 3.3-3.4 ppm (signal *k* in Figure 4.1B) and δ 4.7 (signal *i* in Figure 4.1B), indicating the successful ring-opening reactions of thiolactone moiety in the copolymers. In addition, the results from FTIR were also in good agreement with those obtained from ^{1}H NMR (Supplementary material Figure S4).

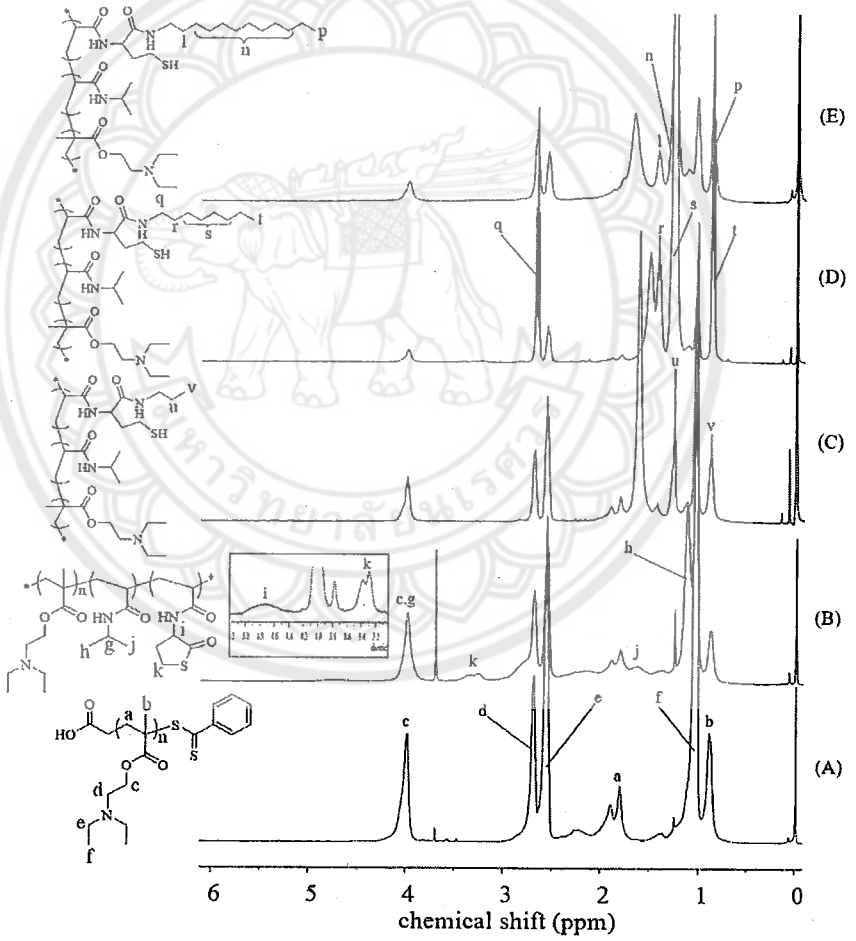

Figure 4.1 ^{1}H NMR spectra of (A) PDEAEMA macro CTA, (B) PDEAEMA-*b*-P(NIPAAm-*st*-TlaAm) copolymers before the ring-opening reaction, and after the ring-opening reactions with (C) 1-propylamine, (D) 1-octylamine, and (E) 1-dodecylamine

After the ring-opening reaction of thiolactone rings in the copolymers with alkylamines to form thiol groups (-SH), the acrylamide-coated MNP was subsequently added to the mixture allowing for the thiol-ene reaction (Lowe 2010). The proposed thiol-ene reaction mechanism between the acrylamide on the MNP surface and thiol groups (-SH) of the copolymer is shown in Figure 4.2. Figure 4.3 shows FTIR spectra of the acrylamide-coated MNP and the MNP coated with the copolymers after the thiol-ene reaction. The signal at 590 cm^{-1} corresponding to Fe-O bond in the MNP appeared in every sample (Figure 4.3). Figure 4.3B-4.3D show the characteristic adsorption signals of C=O stretching (1730 cm^{-1}), C-O stretching (1260 cm^{-1}) of carboxyl groups and C-C stretching (800 cm^{-1}) of the copolymer, signifying the existence of the copolymer on the particle surface through the thiol-ene reaction.

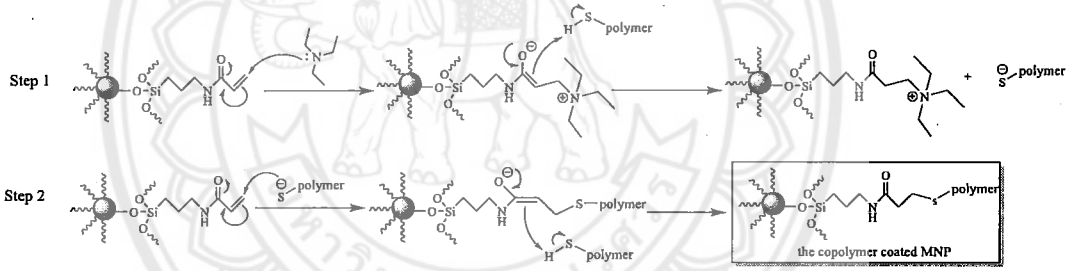

Figure 4.2 The thiol-ene reaction mechanism between the acrylamide groups on the MNP surface and thiol groups of the copolymer

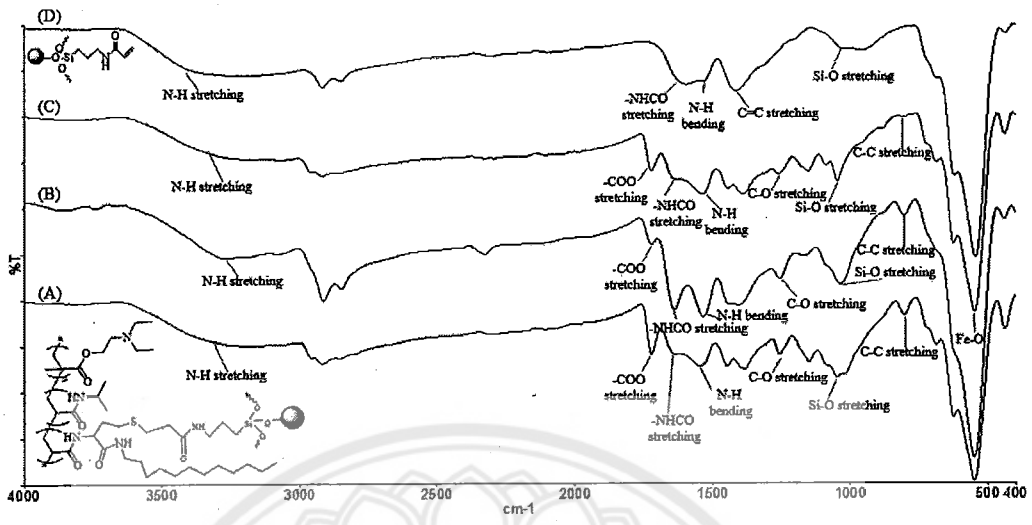

Figure 4.3 FTIR spectra of (A) acrylamide-coated MNP, (B) MC3, (C) MC8, and (D) MC12

To study the organic/inorganic composition of the copoymer-coated MNP, TGA was used to determine the weight loss at 800 $^{\circ}$C (Figure 4.4A). It was hypothesized that the residue weight was the weight of iron oxide from oxidized MNP, while the loss weight was the organic conponents in the copolymer-MNP assemblies. The decrease of the residual weight in the samples corresponded to the increase in the organic contents in the MNP. It was found that there was about 12% organic content in acrylamide-coated MNP, while after coating with the copolymer, there were 26%, 28% and 41% of the polymers in MC12, MC8 and MC3, respectively, signifying that MC3 had higher degree of alkyl substitution as compared to the other two. This was rationalized that the short alkyl chain length in the C3 copolymer might have less steric hindrance in the particle coating step, resulting in the better accessibility of the particles to react with the copolymers and thus higher amounts of the copolymers on the particles.

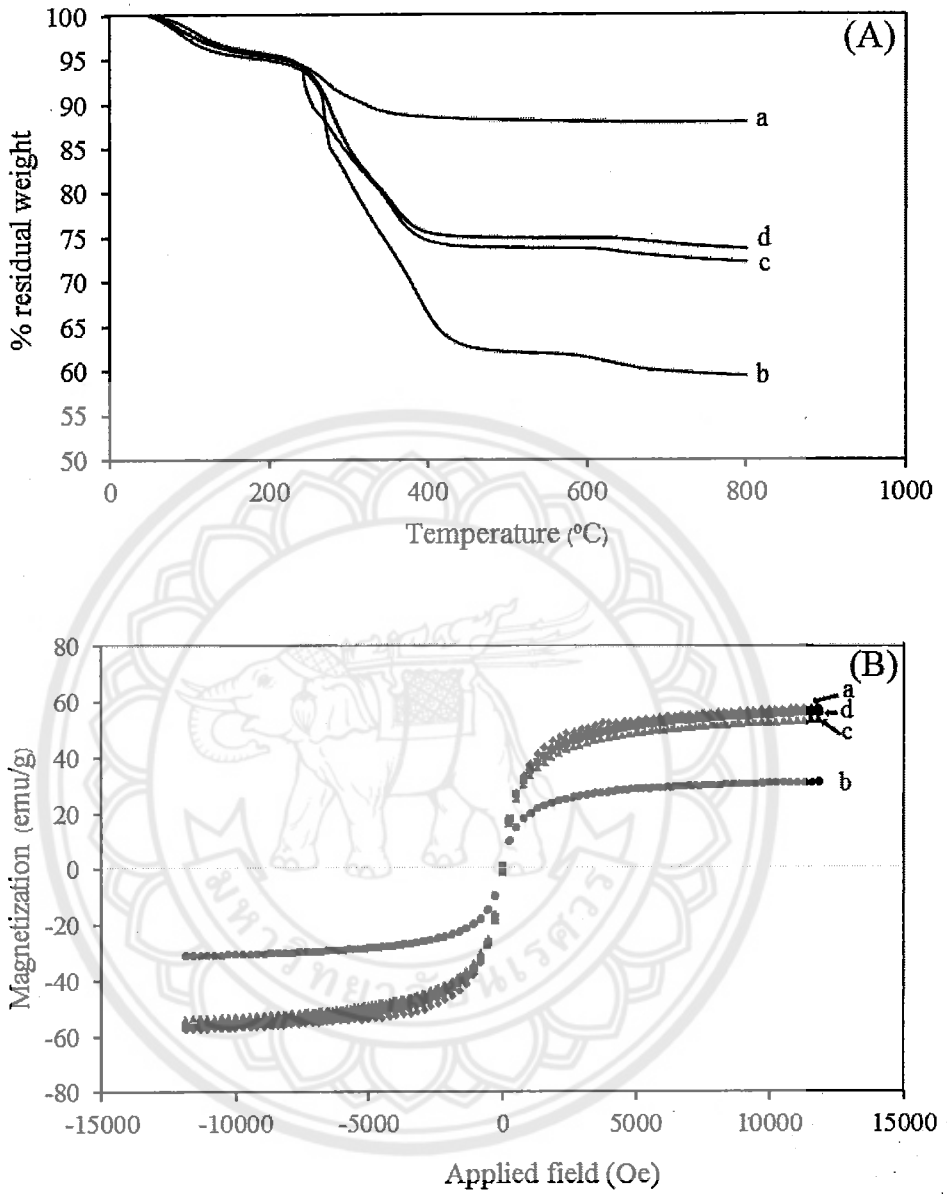

Figure 4.4 (A) TGA thermograms and (B) *M-H* curves of (a) acrylamide-coated MNP, (b) MC3, (c) MC8 and (d) MC12

VSM technique was used to determine magnetic properties of the MNP before and after the copolymer coating (Figure 4.4B). They well responded to an applied magnet and showed superparamagnetic behavior due to the absence of the coercitivity (H_c) and remanence (M_r) upon removal of an external magnetic field. The

saturation magnetization (M_s) decreased from 58 emu/g of acrylamide-coated MNP to 56 emu/g of MC12, 54 emu/g of the MC8 and 31 emu/g of MC3, due to the presence of non-magnetic copolymer on the particle surface and thus the drop of their magnetic responsiveness. The decrease in the net magnetization corresponded well to the increase of the copolymers coated on the particles observed in TGA.

The copolymer-coated MNP was then quaternized to improve the particle dispersibility in water. Zeta potentials of the particle both before (MC3, MC8 and MC12) and after quaternization (qMC3, qMC8, and qMC12) were studied using PCS (Table 4.1). The zeta potentials of acrylamide-coated MNP before and after quaternization did not change because there was no copolymer coated on the MNP surface. After the copolymer coating, their zeta potential values of all copolymers significantly increased from 0 to 16-28 mV after quaternizations, owing to the formation of permanent positive charges of quaternary ammonium groups in the copolymer-coated MNP. It should be noted that these positive charges might facilitate the particles to be well dispersible in an aqueous media, which was necessary for the use in drug controlled release applications discussed later in this report.

In addition, the preliminary studies in the use of the cationic MNP for ionic adsorption with negative bio-entities were also investigated. DNA tagged with 6-carboxytetramethyl rhodamine (TAMRA-5'-TACCACCATTC-3') was selected as a model compound to proof the idea of ionic adsorption capability of the particles. qMC12 (2 mg) as a representative was dispersed in 0.4 μM DNA solution (2 ml) and then stirred for 2 h, followed by magnetic separation. It was found that the concentrations of DNA in the solutions significantly decreased from 0.42 μM to 0.05 μM (Supplementary materials Figure S5), indicating that the MNP can be used as a cationic platform for adsorption with DNA through the electrostatic interaction.

Table 4.1 Zeta potential values and hydrodynamic size (D_h) of the copolymer-coated MNP

Types of MNP	Zeta potential [mV]		D_h of quaternized particles [nm]	
	Before quaternization	After quaternization	at 25 °C	at 45 °C
Acrylamide-coated MNP	-15.3 ± 0.5	-15.3 ± 0.5	564 ± 63	506 ± 52
MC3	0	28.4 ± 1.0	1068 ± 197	396 ± 58
MC8	0	16.2 ± 0.6	836 ± 214	372 ± 103
MC12	0	26.3 ± 0.8	1426 ± 218	295 ± 0

Representative TEM images of acrylamide-coated MNP and the quaternized copolymer-coated MNP (qMC) prepared from aqueous dispersions are shown in Figure 4.5. Acrylamide-coated MNP showed macroscopic aggregation due to the lack of polymer coating resulting in the particles with poor water dispersibility (Figure 4.5A). After coating with the copolymer and then quaternization, formation of the nanoclusters with the size below 200 nm/cluster was observed (Figure 4.5B-4.5D). They showed good dispersibility in water without noticeable aggregation after standing for 2 h (Figure 4.6A). After 75 h, the qMC3 dispersion exhibited some aggregation, while those of qMC8 and qMC12 were insignificant. This was attributed to the higher degree of alkyl substitution of 1-propylamine in the copolymer due to less steric hindrance as compared to those of 1-octyl and 1-dodecylamines, resulting in the higher degree of hydrophobicity of the copolymer and consequently aggregating in water. The TGA result discussed above also supported this assumption that there was higher amount of the copolymer in qMC3, which might result in the higher degree of hydrophobicity as compared to qMC8 and qMC12.

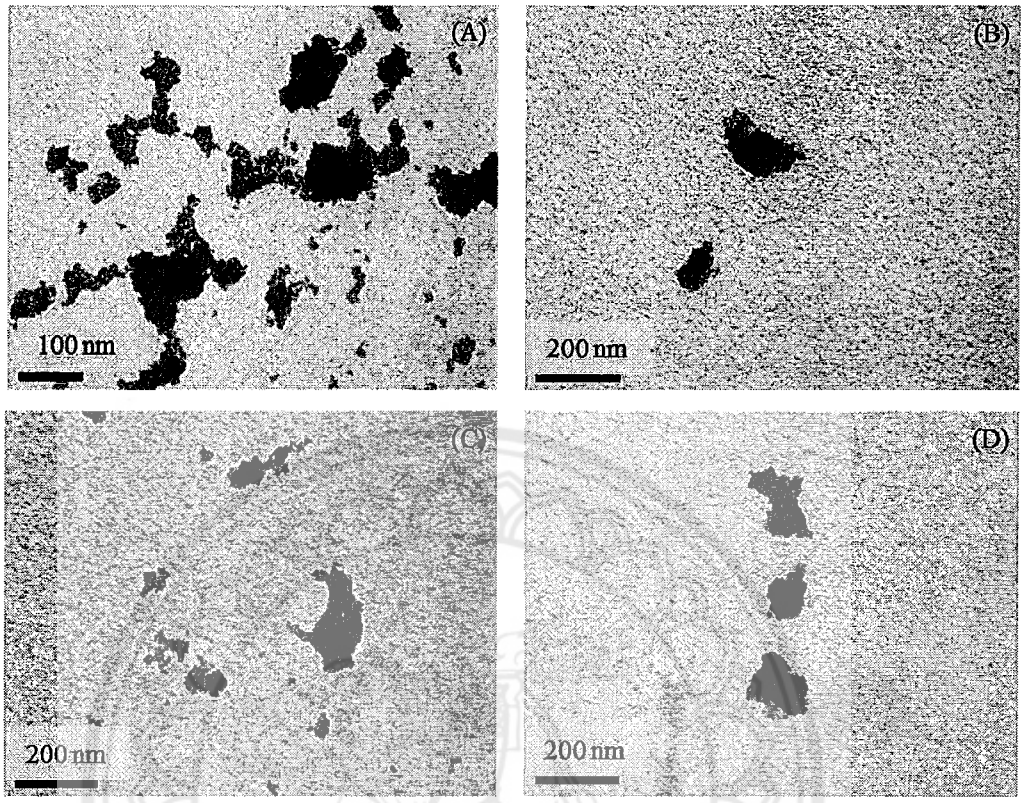

Figure 4.5 TEM images of (A) acrylamide-coated MNP, (B) qMC3, (C) qMC8 and (D) qMC12 prepared from aqueous dispersions

The particle dispersibility in water shown Figure 4.6A was in good agreement with their magnetic separation ability in water. After 5 min of magnetic separation, qMC3 can be completely separated while there were some dispersible particles remaining in qMC8 and qMC12 dispersions (Figure 4.6B). Importantly, the completely separated ability of particles from the dispersion with an assistance of a magnet was necessary for the determination of the drug controlled release discussed later in this work.

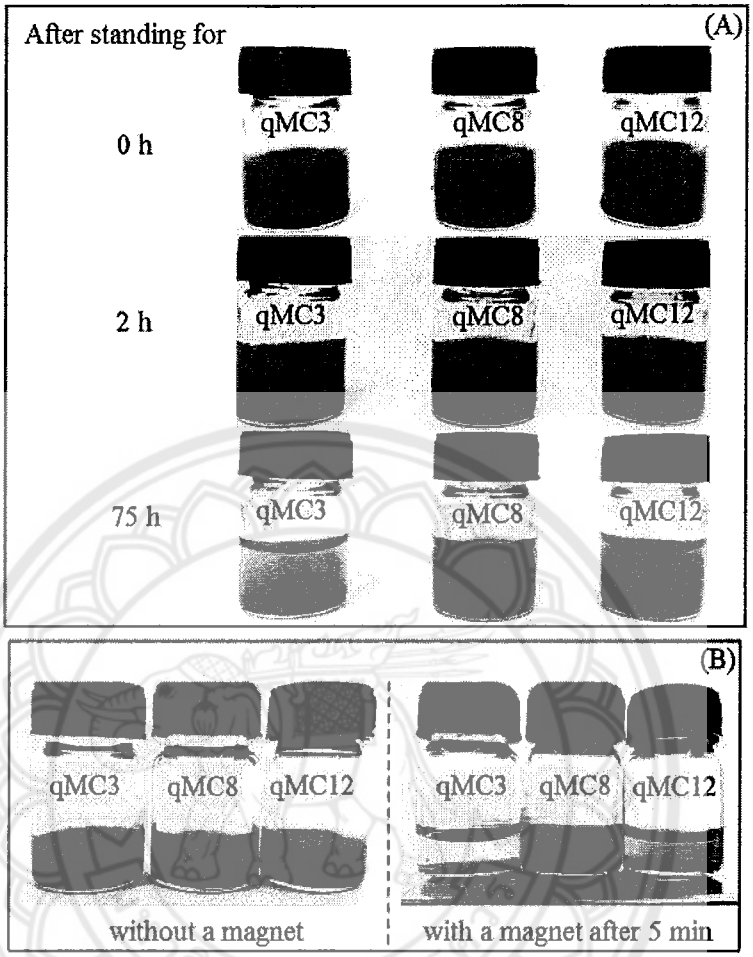

Figure 4.6 (A) Water dispersibility and (B) magnetic separation ability of qMC3, qMC8 and qMC12

Because the copolymer coated on the particles in this work comprised thermo-responsive moieties of PNIPAAm and PDEAEMA, the effect of the change in the temperature on their D_h was investigated. The experimental temperatures were set at 25 °C and 45 °C, which crosses their critical solution temperature (LCST of PNIPAAm = 30-34 °C and LCST of PDEAEMA = 31 °C) [27, 60]. It was found that, in all cases, D_h of the particle coated with the copolymers at 45 °C was smaller than those at 25 °C (Table 4.1). The copolymers collapsed at the temperature above its critical solution temperature, resulting in the shrinkage of the nanocluster and thus the

decrease in their D_h. It should be noted that the shrinkage of the copolymer when heated to 45 °C would be utilized as a triggering mechanism for drug controlled release discussed in the later section.

In vitro release studies of entrapped DOX from the copolymer-coated MNP triggered by the temperature change

DOX, known as a chemotherapy medication used to treat cancer, was used as a model drug for entrapment in and then release from the copolymer-coated MNP. Fluorescence spectra of the DNA solutions before and after adsorption with qMC12 and (B) a standard calibration curve of the DNA solutions (TAMRA-5'-TACCACCATTC-3') are shown in Figure S6 (in the supplementary materials). It was hypothesized that DOX was entrapped in the copolymer-coated particles due to the hydrogen bonding of DOX molecules with the copolymer. %EE of qMC3 was *ca.*5.4%, while those of qMC8 and qMC12 ranged between 10.3% and 10.8%. The two-fold lower percentage of qMC3 as compared to those of the other two samples was probably due to the higher degree of hydrophobicity in qMC3 (higher degree of alkyl substitution), which might result in less entrapment of DOX on the particles.

DOX release studies were performed at 25 °C with a step-wise increase in the temperature to 45 °C after the equilibrium (Figure 4.7). In all cases, the release of DOX from the particle at 25 °C reached their equilibrium within 40 min and they were held at this temperature for 1 h to ensure the equilibrium. Generally, when the temperature of dispersion is increased above room temperature, the preloaded drug should mainly be released *via* a diffusion mechanism [61]. In this work, when increasing the temperature to 45 °C (above LCST of PNIPAAm), all samples (qMC3, qMC8 and qMC12) showed the same trend of the drug release. The increment of DOX release upon increasing the temperature was mainly attributed to "a diffusion mechanism". Interestingly, qMC8 and qMC12 showed the faster rate of DOX release with additional release of *ca.*8-10% and reached the equilibrium within 40 min. This accelerated release rate was attributed to "a squeezing mechanism" due to the

collapse of PNIPAAm chains at above its LCST [62]. However, the release rate of DOX in qMC3 seemed to be retarded at the beginning of the elevated temperature and it was then slowly released afterward with additional DOX release of *ca.*11%. The higher degree of hydrophobicity in qMC3 discussed above might inhibit the squeezing behavior of PNIPAAm in the copolymer, which thus initially retarded the release of the entrapped drug from the particles at the elevated temperature (Figure 4.8).

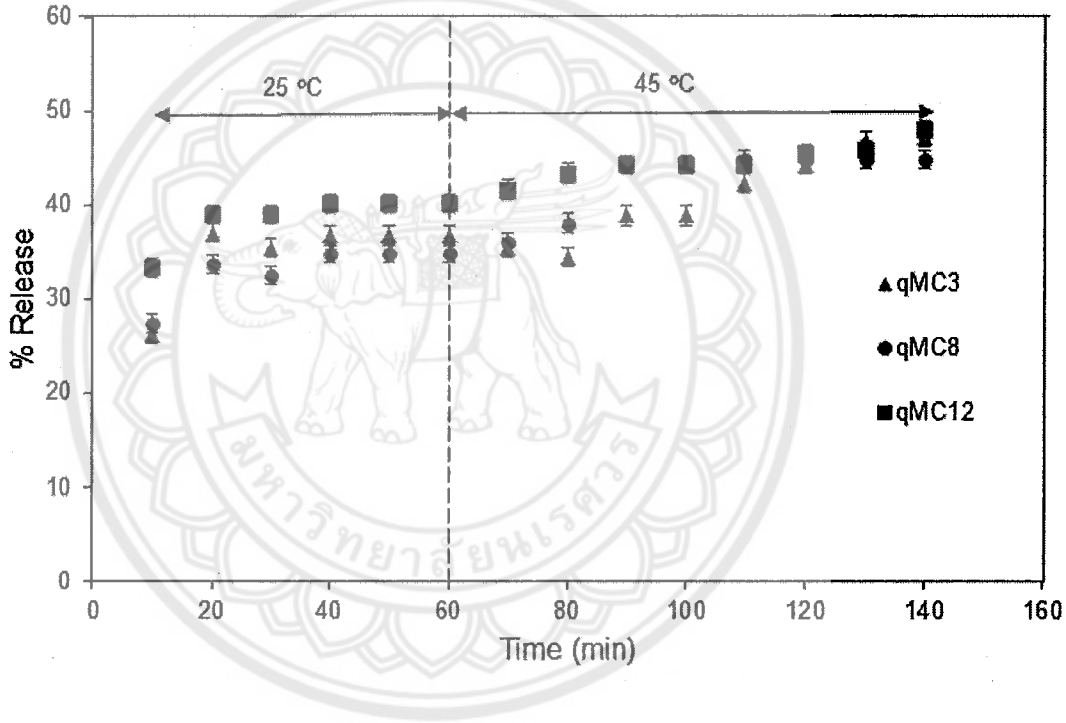

Figure 4.7 DOX release profiles of the copolymer-coated MNP (qMC3, qMC6 and qMC12)

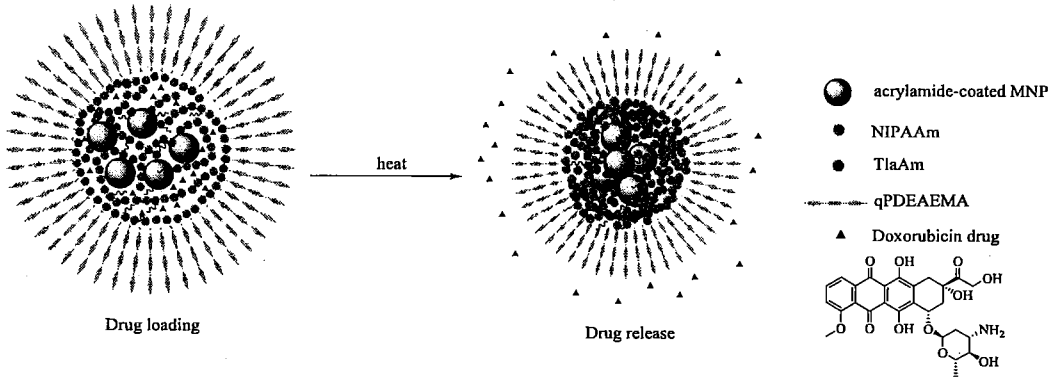

Figure 4.8 The proposed mechanism of DOX release from the copolymer-coated MNP

CHAPTER V
CONCLUSIONS

We herein reported the multi-responsive MNP modified with cationic PDEAEMA-*b*-P(NIPAAm-*st*-TlaAm) copolymer and its potential applications in controlled drug release and bio-conjugation. Degree of hydrophobicity of the copolymers coated on surface of particle can be tuned by using various alkyl chain lengths in thiolactone ring-opening reaction and this can influence the particle self-assemblies in water (e.g. D_h, dispersibility, nano-aggregation) and the drug release rate. These particles exhibited the temperature responsive behavior, which can be used as a triggering mechanism for controlled release of DOX. These versatile copolymer-MNP assemblies showed an enormous potential for use as a smart platform with thermal-triggering controlled drug release system and for conjugation with any negatively charged bio-entities.

REFERENCES

[1] B. Sahoo, K. S. P. Devi, R. Banerjee, T. K. Maiti, P. Pramanik, D. Dhara, Thermal and pH responsive polymer-tethered multifunctional magnetic nanoparticles for targeted delivery of anticancer drug, ACS Appl. Mater. Interfaces. 5 (2013) 3884–3893.

[2] C. Wang, H. Xu, C. Liang, Y. Liu, Z. Li, G. Yang, et al, Iron oxide @ polypyrrole nanoparticles as a multifunctional drug carrier for remotely controlled cancer therapy with synergistic antitumor effect, ACS nano. 7 (2013) 6782–6795.

[3] Y. Li, X. Zhang, H. Cheng, G. Kim, S. Cheng, R. Zhuo, Novel stimuli-responsive micelle self-assembled from Y-Shaped P(UA-Y-NIPAAm) copolymer for drug delivery, Biomacromolecules. 7 (2006) 2956–2960.

[4] W. E. Mahmoud, L. M. Bronstein, F. Al-Hazmi, F. Al-Noaiser, A. A. Al-Ghamdi, Development of Fe/Fe_3O_4 core–shell nanocubes as a promising magnetic resonance imaging contrast agent, Langmuir. 16 (1999) 3–27.

[5] Y. Hu, L. Meng, L. Niu, Q. Lu, Highly cross-linked and biocompatible polyphosphazene-coated superparamagnetic Fe_3O_4 nanoparticles for magnetic resonance imaging, Langmuir. 29 (2013) 9156–9163.

[6] Y. Qu, J. Li, J. Ren, J. Leng, C. Lin, D. Shi, Enhanced magnetic fluid hyperthermia by micellar magnetic nanoclusters composed of Mn_xZn_1–xFe_2O_4 nanoparticles for induced tumor cell apoptosis, J. Am. Chem. Soc. 6 (2014) 16867–16879.

[7] L. Chen, H. Zhang, L. Li, Y. Yang, X. Liu, B. Xu, Thermoresponsive hollow magnetic microspheres with hyperthermia and controlled release properties, J. Appl. Polym. Sci. 10 (2015) 42617–42626.

[8] L. P. Singh, S. K. Srivastava, R. Mishra, R. S. Ningthoujam, Multifunctional hybrid nanomaterials from water dispersible $CaF_2:Eu^{3+}$, Mn^{2+} and Fe_3O_4 for

luminescence and hyperthermia application, J. Phys. Chem. 118 (2014) 18087–18096.

[9] J. Lim, S. P. Yeap, H. X. Che, S. C. Low, Characterization of magnetic nanoparticle by dynamic light scattering, Nanoscale Res. Lett. 8 (2013) 381–394.

[10] J. T. Chen, M. Ahmed, Q. Liu, R. Narain, Synthesis of cationic magnetic nanoparticles and evaluation of their gene delivery efficacy in Hep G2 cells, J Biomed Mater Res A. 100A (2012) 2342–2347.

[11] S. Mekkapat, B. Thong-On, B. Rutnakornpituk, U. Wichai, M. Rutnakornpituk, Magnetic core–bilayer shell complex of magnetite nanoparticle stabilized with mPEG–polyester amphiphilic block copolymer, J. Nanopart. Res. 15 (2013) 2051–2062.

[12] K. C. F. Leung, S. Lee, C. Wong, C. Chak, J. M. Y. Lai, X. Zhu, Y. J. Wang, Y. X. J. Wang, C. H. K. Cheng, Nanoparticle–DNA–polymer composites for hepatocellular carcinoma cell labeling, sensing, and magnetic resonance imaging, Methods. 64 (2013) 315–321.

[13] N. Machida, Y. Inoue, K. Ishihara, Phospholipid polymer-coverd magnetic nanoparticles for tracking intracellular molecular reaction, Trans. Mat. Res. Soc. Japan. 39 (2014) 427–430.

[14] G. Prabha, V. Raj, Preparation and characterization of polymer nanocomposites coated magnetic nanoparticles for drug delivery applications, J. Magn. Magn. Mater. 408 (2016) 26–34.

[15] K. Ulbrich, K. Holá, V. Šubr, A. Bakandritsos, J. Tuček, R. Zbořil, Targeted drug delivery with polymers and magnetic nanoparticles: covalent and noncovalent approaches, release control, and clinical studies, Chem. Rev. 116 (2016) 5338–5431.

[16] S. Qin, D. Qin, W. T. Ford, D. E. Resasco, J. E. Herrera, Functionalization of single-walled carbon nanotubes with polystyrene *via* grafting to and grafting from methods, Macromolecules. 37 (2004) 752–757.

[17] B. Wang, B. Li, B. Zhao, C. Y. Li, Amphiphilic janus gold nanoparticles *via* combining "solid-state grafting-to" and "grafting-from" methods, J. Am. Chem. Soc. 130 (2008) 11594–11595.

[18] W. A. Braunecker, K. Matyjaszewski, Controlled/living radical polymerization: features, developments, and perspectives, Prog. Polym. Sci. 32 (2007) 93–146.

[19] K. Matyjaszewski, Controlled radical polymerization: state-of-the-art in 2014, J. Am. Chem. Soc, v1187, 2015. http://dx.doi.org/10.1021/bk-2015-1187.ch001.

[20] V. Sciannamea, R. Je´ro^me, C. Detrembleur, In-situ nitroxide-mediated radical polymerization (NMP) processes: their understanding and optimization, Chem. Rev. 108 (2008) 1104-1126.

[21] G. Moad, E. Rizzardo, Nitroxide mediated polymerization: from fundamentals to applications in materials science, Polym. Chem, v19, 2016. http://dx.doi.org/10.1039/9781782622635.

[22] K. Matyjaszewski, Atom transfer radical polymerization (ATRP): current status and future perspectives, Macromolecules. 45 (2012) 4015–4039.

[23] L. Huang, M. Liu, L. Mao, D. Xu, Q. Wan, G. Zeng, et al, Preparation and controlled drug delivery applications of mesoporous silica polymer nanocomposites through the visible light induced surface-initiated ATRP, Appl. Surf. Sci. 412 (2017) 571–577.

[24] G. Moad, E. Rizzardo, S. H. Thang, Radical Addition Fragmentation Chemistry in Polymer Synthesis, Polymer. 49 (2008) 1079–1131.

[25] M. R. Hill, R. N. Carmean, B. S. Sumerlin, Expanding the scope of RAFT polymerization: recent advances and new horizons, Macromolecules. 48 (2015) 5459–5469.

[26] H. Willcock, R. K. O'Reilly, End group removal and modification of RAFT polymers, Polym. Chem. 1 (2010) 149–157.

[27] A. Gandhi, A. Paul, S. O. Sen, K. K. Sen, Studies on thermoresponsive polymers: phase behaviour, drug delivery and biomedical applications, Asian J. Pharmacol. 10 (2015) 99–107.

[28] H. Du, R. Wickramasinghe, X. Qian, Effects of salt on the lower critical solution temperature of poly (N-isopropylacrylamide), J. Phys. Chem. 114 (2010) 16594–16604.

[29] I. Bischofberger, V. Trappe, New aspects in the phase behaviour of poly-N-isopropyl acrylamide: systematic temperature dependent shrinking of PNiPAM assemblies well beyond the LCST, Sci. Rep. 5 (2015) 15520–15529.

[30] S. S. Patil, P. P. Wadgaonkar, Temperature and pH dual stimuli responsive PCL-*b*-PNIPAAm block copolymer assemblies and the cargo release studies, J. Polym. Sci. A Polym. Chem. 55 (2017) 1383–1396.

[31] N. Rodkate, M. Rutnakornpituk, Multi-responsive magnetic microsphere of poly(N-isopropylacrylamide)/carboxymethylchitosan hydrogel for drug controlled release, Carbohydr. Polym. 151 (2016) 251–259.

[32] S. Meerod, B. Rutnakornpituk, U. Wichai, M. Rutnakornpituk, Hydrophilic magnetic nanoclusters with thermo-responsive properties and their drug controlled release, J. Magn. Magn. Mater. 392 (2015) 83–90.

[33] P. Espeel, F. E. Du Prez, One-pot multi-step reactions based on thiolactone chemistry: a powerful synthetic tool in polymer science, Eur. Polym. J. 6 (2015) 2247–272.

[34] M. M. Stamenovi, P. Espeel, V. Van Camp, F. E. Du Prez, Norbornenyl-based RAFT agents for the preparation of functional polymers *via* thiol-ene chemistry, Macromolecules. 44 (2011) 5619–5630.

[35] P. Espeel, F. Goethals, M. M. Stamenovi, L. Petton, F. E. Du Prez, Double modular modification of thiolactone-containing polymers: towards polythiols and derived structures, Polym. Chem. 3 (2012) 1007–1015.

[36] Y. Chen, P. Espeel, S. Reinicke, F. E. Du Prez, M. H. Stenzel, Control of glycopolymer nanoparticle morphology by a one-pot, double modification procedure using thiolactones, Macromol. Rapid Commun. 35 (2014) 1128–1134.

[37] S. Reinicke, P. Espeel, M. M. Stamenović, F. E. Du Prez, One-pot double modification of P(NIPAAm): a tool for designing tailor-made multiresponsive polymers, ACS Macro Lett. 2 (2013) 539–543.

[38] P. Espeel, F. Goethals, F. E. Du Prez, One-pot multistep reactions based on thiolactones: extending the realm of thiol-ene chemistry in polymer synthesis, J. Am. Chem. Soc. 133 (2011) 1678–1681.

[39] M. A. Ward, T. K. Georgiou, Thermoresponsive polymers for biomedical applications. Polymers, 3 (2011) 1215-1242.

[40] L. Klouda, A. G. Mikos, Thermoresponsive hydrogels in biomedical applications, Euro. J. Pharm. Biopharm. 68 (2008) 34-45.

[41] J. F. Lutz, Polymerization of oligo(ethylene glycol) (meth)acrylates: toward new generations of smart biocompatible materials, J. Polym. Sci. Pol. Chem. 46 (2008) 3459-3470.

[42] N. T. Southall, K. A. Dill, A. D. J. Haymet, A view of the hydrophobic effect, J. Phys. Chem. B. 106 (2002) 521-533.

[43] C. Vasile, A. K. Kulshreshtha, (2003). Handbook of Polymer Blends and Composites. Shawbury, UK; Rapra Technology.

[44] Z. P. Zhao, Z. Wang, S. C. Wang, Formation, charged characteristic and BSA adsorption behavior of carboxymethyl chitosan/PES composite MF membrane, J. Membrane Sci. 217 (2003) 151-158.

[45] Q. Mu, Y. Fang, Preparation of thermosensitive chitosan with poly(*N*-isopropylacrylamide) side at hydroxyl group *via* *O*-maleoyl-*N*-phthaloyl-chitosan (MPCS), Carbohyd. Polym. 72 (2008) 308-314.

[46] Y. Cao, C. Zhang, W. Shen, Z. Cheng, L. Yu, Q. Ping, Poly(*N*-isopropylacrylamide)-chitosan as thermosensitive *in situ* gel-forming system for ocular drug delivery, J. Control. Release. 120 (2007) 186-194.

[47] P. Glampedaki, J. Krägel, G. Petzold, V. Dutschk, R. Miller, M. M. C. G. Warmoeskerken, Polyester textile functionalisation through incorporation of pH/thermo-responsive microgels. Part I: Microgel preparation and characterization, Colloid. Surface. A. 47(5) (2012) 2078-2087.

[48] J. P. Chen, S. H. Chiu, A poly(*N*-isopropylacrylamide-*co*-*N*-acryloxysuccinimide-*co*-2-hydroxyethyl methacrylate) composite hydrogel membrane for urease immobilization to enhance urea hydrolysis rate by temperature swing, Enzyme. Microb. Tech. 26 (2000) 359-367.

[49] Z.M.O. Rzaev, S. Dincer, E. Piskin, Functional copolymers of *N*-isopropylacrylamide for bioengineering applications, Prog. Polym. Sci. 32 (2007) 534-595.

[50] H. Zhou, F. Liang, J. Li, X. Ding, A. Ma, W. Chen, C. Luo, G. Zhang, W. Tian, M. Cheng, B. Liao, RAFT polymerization and dually responsive behaviors of terpyridine-containing PNIPAAm copolymers in dilute solutions, React. Funct. Polym. 106 (2016) 62-68.

[51] A. L. Barnes, P. G. Genever, S. Rimmer, M. C. Coles, Collagen–poly(N-isopropylacrylamide) hydrogels with tunable properties, Biomacromolecules 17 (2016) 723-734.

[52] T. Fan, M. Li, X. Wu, M. Li, Y. Wu, Preparation of thermoresponsive and pH-sensitivity polymer magnetic hydrogel nanospheres as anticancer drug carriers. Colloid. Surface. B. 88 (2011) 593-600.

[53] S. Belbekhouche, S. Reinicke, P. Espeel, F. E. Du Prez, P. Eloy, C. Dupont-Gillain, A. M. Jonas, S. Demoustier-Champagne, K. Glinel, Polythiolactone-based redox-responsive layers for the reversible release of functional molecules, ACS Appl. Mater. Inter. 6 (2014) 22457.

[54] S. Reinicke, P. Espeel, M. M. Stamenović, F. E. Du Prez, One-pot double modification of p(NIPAAm): a tool for designing tailor-made multiresponsive polymers, ACS Macro. Lett. 2 (2013) 539-543.

[55] Y. Chen, P. Espeel, S. Reinicke, F. E. Du Prez, M. H. Stenzel, Control of glycopolymer nanoparticle morphology by a one-pot, double modification procedure using thiolactones, Macromol. Rapid. Commun. 35 (2014) 1128–1134.

[56] S. Wan, J. Huang, H. Yan, K. Liu, Size-controlled preparation of magnetite nanoparticles in the presence of graft copolymers, J. Mater. Chem. 16 (2006) 298-303.

[57] Q. L. Fan, K. G. Neoh, E.T. Kang, B. Shuter, S.C. Wang, Solvent-free atom transfer radical polymerization for the preparation of poly(poly(ethyleneglycol)

monomethacrylate)-grafted Fe_3O_4 nanoparticles: Synthesis, characterization and cellular uptake, Biomaterials, 28 (2007) 5426-5436.

[58] F. Galeotti, F. Bertini, G. Scavia, A. Bolognesi, A controlled approach to iron oxide nanoparticles functionalization for magnetic polymer brushes. J. Colloid. Interf. Sci. 360 (2011) 540-547.

[59] M. Rutnakornpituk, N. Puangsin, P. Theamdee, B. Rutnakornpituk, U. Wichai, Poly(acrylic acid)-grafted magnetic nanoparticle for conjugation with folic acid, Polymer, 52 (2011) 987-995.

[60] Y. Maeda, H. Mochiduki, Hydration changes during thermosensitive association of a block copolymer consisting of LCST and UCST blocks, Macromol. Rapid. Commun. 25 (2004) 1330–1334.

[61] P. Liu, Q. Luo, Y. Guan, Y. Zhang, Drug release kinetics from monolayer films of glucose-sensitive microgel, Polymer 51 (2010) 2668-2675.

[62] T. Trongsatitkul, B. M. Budhlall. Microgels or microcapsules? Role of morphology on the release kinetics of thermoresponsive PNIPAm-co-PEGMa hydrogels, Polym. Chem 4 (2013) 1502-1516.

APPENDIX A

Supplementary Material

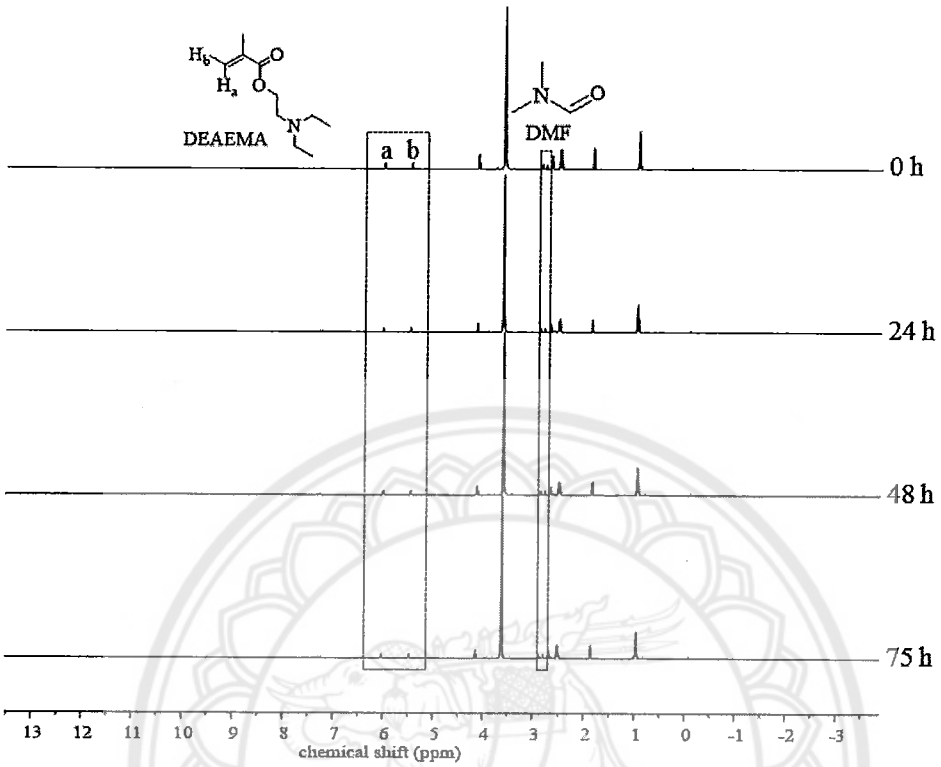

Figure S1 Monitoring the monomers conversions *via* ^{1}H NMR spectroscopy during RAFT of DEAEMA using DMF as an internal standard

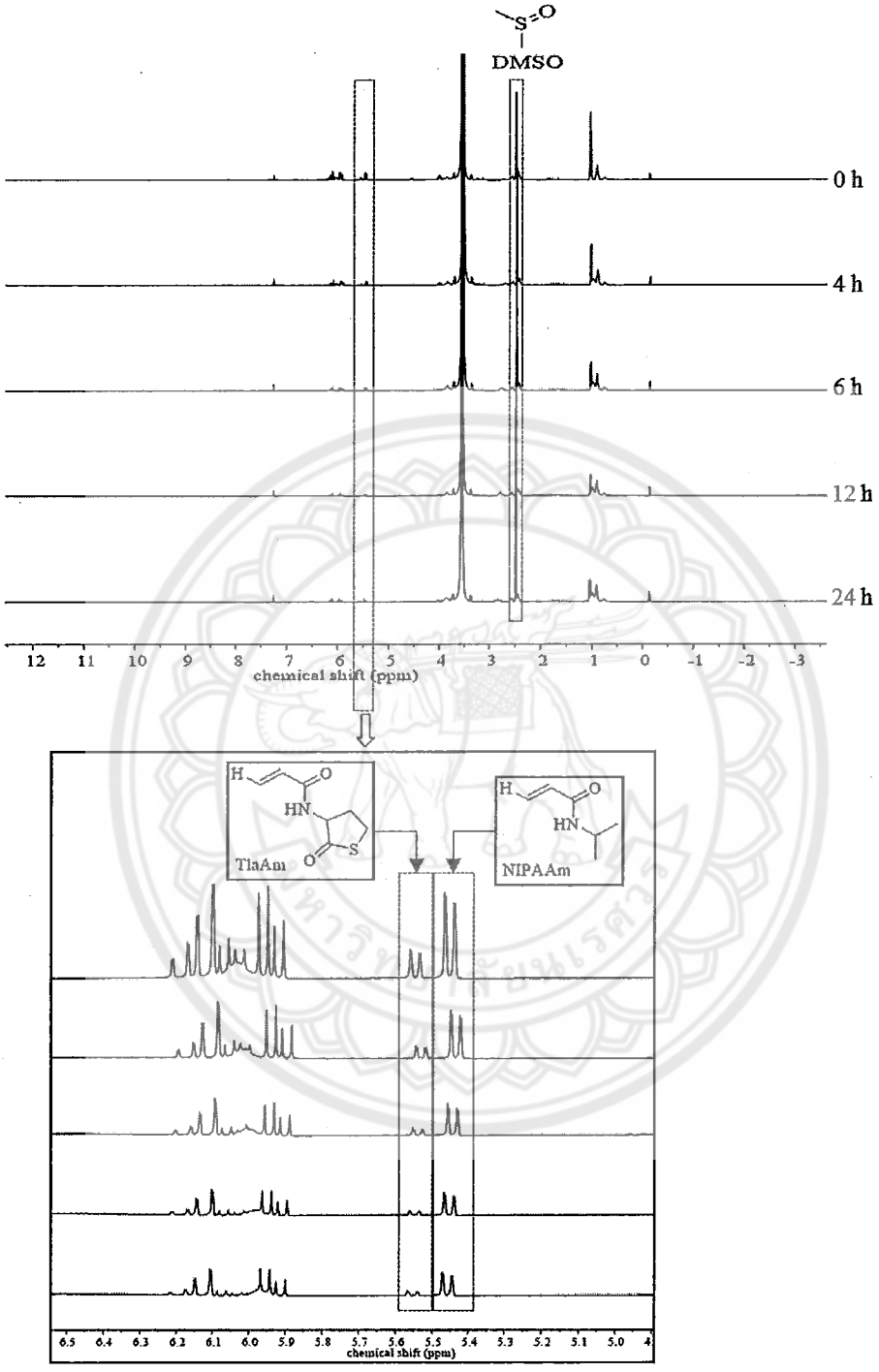

Figure S2 Monitoring the monomers conversions of PDEAEMA-*b*-P(NIPAAm-*st*-TlaAm) *via* ^{1}H NMR spectroscopy during RAFT using DMF as an internal standard

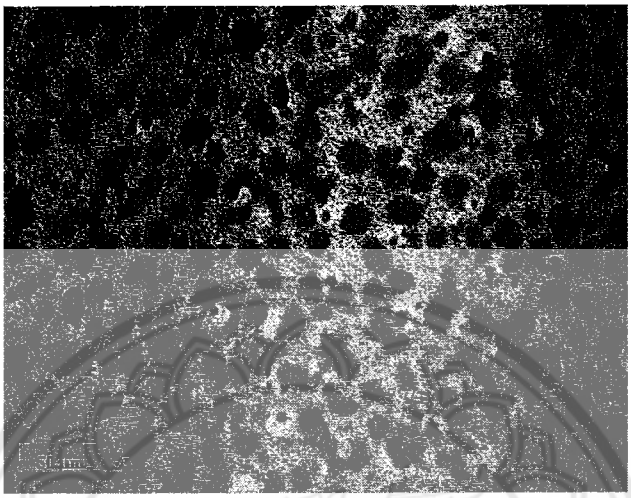

Figure S3 A TEM image of quaternized C12 copolymer showing the self-assemble behavior. The TEM sample was prepared from the copolymer aqueous dispersion.

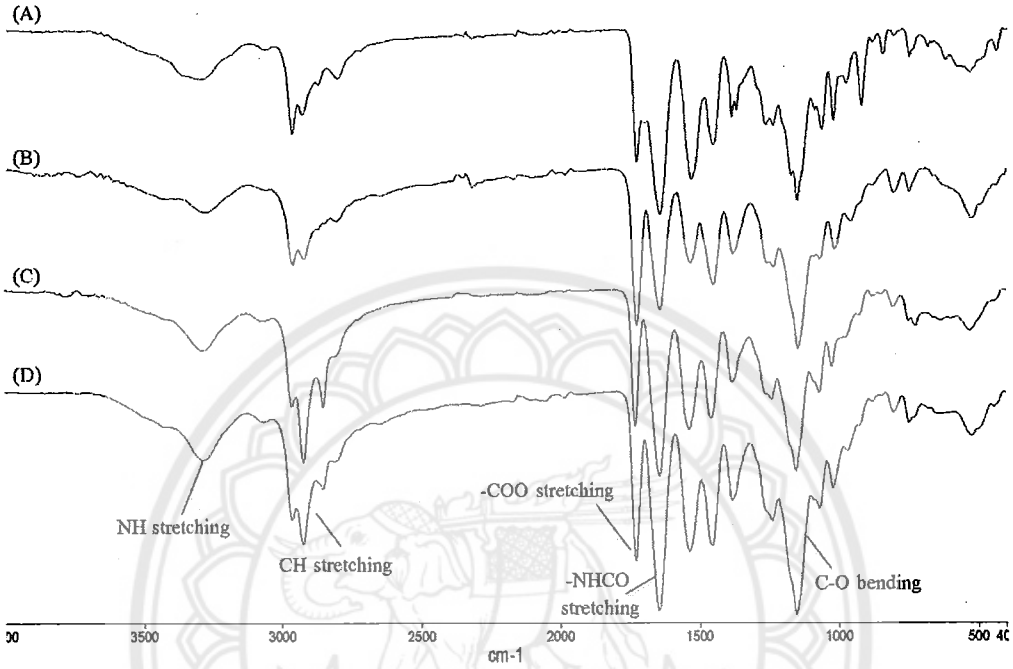

Figure S4 FTIR spectra of (A) PDEAEMA-*b*-P(NIPAAm-*st*-TlaAm) copolymers before the ring-opening reaction, and after the ring-opening reactions with (B) 1-propylamine, (C) 1-octylamine, and (D) 1-dodecylamine

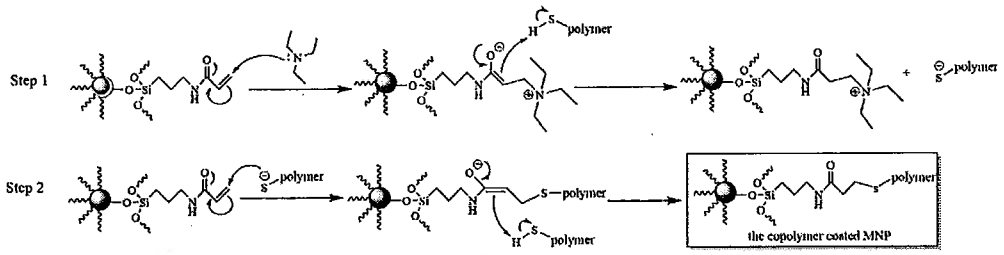

Figure S5. The thiol-ene reaction mechanism between the acrylamide groups on the MNP surface and thiol groups of the copolymer

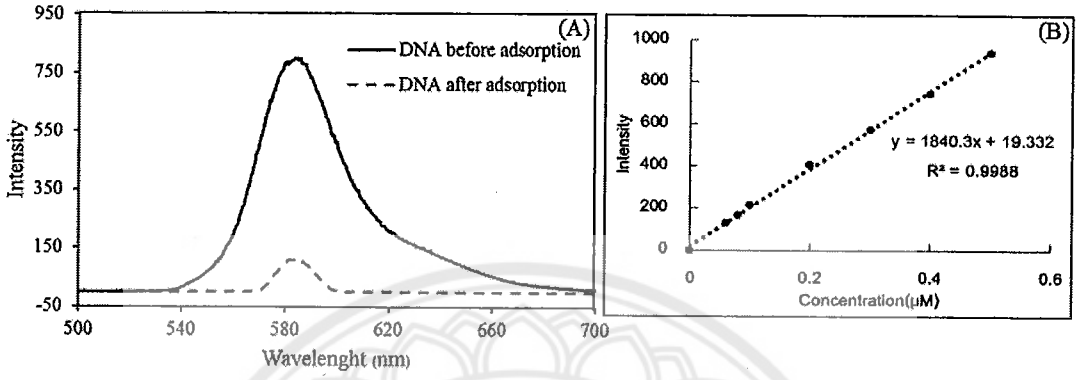

Figure S6 (A) Fluorescence spectra of the DNA solutions before and after adsorption with qMC12 and (B) a standard calibration curve of the DNA solutions (TAMRA-5'-TACCACCATTC-3')

Appendix B

ตารางเปรียบเทียบกิจกรรมที่เสนอในข้อเสนอโครงการ
และกิจกรรมที่ทำจริงและตารางเปรียบเทียบ output ที่เสนอใน
ข้อเสนอโครงการและที่ได้จริง

ตารางเปรียบเทียบกิจกรรมที่เสนอในข้อเสนอโครงการและกิจกรรมที่ทำจริง

วัตถุประสงค์	กิจกรรมที่วางแผนไว้	กิจกรรมที่ได้ดำเนินจริง
1. To modify MNP surface with PDEAEMA-*b*-P(NIPAAm-*st*-TlaAm) copolymer to obtain magnetic nanocluster with bilayer copolymer coating with thermo-responsive properties. 2. To apply the copolymer-coated MNP for use in drug controlled release application. 3. To study the effect of temperature changes on drug releasing behavior of the copolymer-coated MNP.	Step 1: Synthesis of TlaAm monomer	TlaAm monomer was synthesized and characterized via ^{1}H NMR technique.
	Step 2: Synthesis of acrylamide-coated MNP	The acrylamide-coated MNP was synthesized and characterized via FTIR TEM, VSM and TGA techniques
	Step 3: Synthesis of PDEAEMA macro CTA	PDEAEMA macro CTA was synthesized and characterized via ^{1}H NMR technique.
	Step 4: Synthesis of PDEAEMA-b-P(NIPAAm-st-TlaAm) block copolymer	PDEAEMA-b-P(NIPAAm-st-TlaAm) block copolymer were synthesized and characterized via ^{1}H NMR technique.
	Step 5: Synthesis of the copolymer-coated MNP	The copolymer-coated MNP were synthesized and characterized via FTIR, TEM, VSM, PCS and TGA techniques
	Step 6: Quaternization of PDEAEMA in the copolymer-coated MNP	The copolymer-coated MNP was quaternized and characterized via PCS technique.
	Step 7: In vitro release studies of entrapped DOX from the copolymer-coated MNP	In vitro release studies of entrapped DOX from the copolymer-coated MNP was studied as a function of temperature.

ตารางเปรียบเทียบ output ที่เสนอในข้อเสนอโครงการและที่ได้จริง

Output		ในกรณีล่าช้า (ผลสำเร็จไม่ถึง 100%) ให้ท่านระบุสาเหตุและการแก้ไขที่ท่านดำเนินการ
กิจกรรมในข้อเสนอโครงการ/หรือจากการปรับแผน	ผลสำเร็จ (%)	
Step 1: Synthesis of TlaAm monomer	100%	-
Step 2: Synthesis of acrylamide-coated MNP	100%	-
Step 3: Synthesis of PDEAEMA macro CTA	100%	-
Step 4: Synthesis of PDEAEMA-b-P(NIPAAm-st-TlaAm) block copolymer	100%	-
Step 5: Synthesis of the copolymer-coated MNP	100%	-
Step 6: Quaternization of PDEAEMA in the copolymer-coated MNP	100%	-
Step 7: In vitro release studies of entrapped DOX from the copolymer-coated MNP	100%	-

Appendix C

เผยแพร่ผลงานวารสารระดับนานาชาติที่มีค่า impact factor

S. Paenkaew and M. Rutnakornpituk

Effect of alkyl chain lengths on the assemblies of magnetic nanoparticles coated with multi-functional thiolactone-containing copolymer

Journal of Nanoparticle Research (2018) 20, 193-204 (IF 2.127, year 2017)

J Nanopart Res (2018) 20:193
https://doi.org/10.1007/s11051-018-4295-2

RESEARCH PAPER

Effect of alkyl chain lengths on the assemblies of magnetic nanoparticles coated with multi-functional thiolactone-containing copolymer

Sujittra Paenkaew · Metha Rutnakornpituk

Received: 8 March 2018 / Accepted: 5 July 2018

Abstract This work presents the synthesis of magnetite nanoparticle (MNP) coated with poly(N,N-diethylaminoethyl methacrylate)-*b*-poly(N-isopropyl acrylamide-*st*-thiolactone acrylamide) (PDEAEMA-*b*-P(NIPAAm-*st*-TlaAm) copolymer and its use in controlled drug release and bio-conjugation. TlaAm units in the copolymer were ring-opened with various alkyl amines to form thiol groups (-SH), followed by thiol-ene coupling reactions with acrylamide-coated MNP and then quaternized to obtain cationic copolymer-MNP assemblies (the size < 200 nm/cluster). The use of alkyl amines having various chain lengths (e.g., 1-propylamine, 1-octylamine, or 1-dodecylamine) in the nucleophilic ring-opening reactions of the thiolactone rings affected their magnetic separation ability, water dispersibility, and release rate of doxorubicin model drug. In all cases, when increasing the temperature, they showed a thermo-responsive behavior as indicated by the decrease in hydrodynamic size and the accelerated drug release rate. These copolymer-MNP assemblies could be used as a novel platform with thermal-triggering controlled drug release and capability for adsorption with any negatively charged biomolecules.

Keywords Magnetic · Nanoparticle · Assembly · Thiolactone · Thermo-responsive · Polimer coating · Drug delivery

Introduction

In recent years, magnetite nanoparticle (MNP) has extensively attracted interest owing to their superparamagnetic properties and their potential applications in various fields. Incorporation of MNP into various organic nano-assemblies has been investigated by features of their intriguing biomedical applications, such as remotely controlled drug release, magnetically guidable drug delivery (Sahoo et al. 2013; Wang et al. 2013; Li et al. 2006), magnetic resonance imaging (MRI) (Mahmoud et al. 2013; Hu et al. 2013), and hyperthermia cancer treatment delivery (Qu et al. 2014; Chen et al. 2015; Singh et al. 2014). However, it tends to aggregate to each other mainly owing to dipole-dipole and magnetic attractive forces, leading the loss in nano-scale related properties and a decrease in the surface area/volume ratio (Lim et al. 2013). Grafting long-chain polymers onto MNP surface

Electronic supplementary material The online version of this article (https://doi.org/10.1007/s11051-018-4295-2) contains supplementary material, which is available to authorized users.

S. Paenkaew · M. Rutnakornpituk (✉)
Department of Chemistry and Center of Excellence in Biomaterials, Faculty of Science, Naresuan University, Phitsanulok 65000, Thailand
e-mail: methar@nu.ac.th

Published online: 13 July 2018

is currently one of the promising approaches to realize its dispersibility in the media due to charge repulsion of ionic surface or steric repulsion of long chain surfactant (Chen et al. 2012; Mekkapat et al. 2013). In addition, this polymeric coating can also serve as a platform for conjugation of biomolecules of interest on the MNP surface (Leung et al. 2013; Machida et al. 2014; Prabha and Raj 2016; Ulbrich et al. 2016).

Many works have now extensively reported in the MNP polymeric coating accomplished either via "grafting from" or "grafting to" strategies (Qin et al. 2004; Wang et al. 2008) with controlled radical polymerization (CRP) techniques. CRP technique produces well controllable polymer architecture on particle surface because it can control molecular weight, polydispersity, functionality, and composition distribution of polymers (Braunecker and Matyjaszewski 2007). Three general techniques of CRP include nitroxide-mediated polymerization (NMP) (Sciannamea et al. 2008), atom transfer radical polymerization (ATRP) (Matyjaszewski 2012; Huang et al. 2017), reversible addition fragmentation chain transfer polymerization (RAFT) (Moad et al. 2008; Hill et al. 2015). Being of our particular interest, RAFT as opposed to other CRP techniques can be performed in various kinds of solvent, wide range of temperature, no need of metals used for polymerization, and large range of monomer classes (Willcock and O'Reilly 2010).

This present work reports the synthesis of a multifunctional copolymer via RAFT for coating onto the surface of MNP and its use in drug-controlled release and bio-conjugation. This copolymer was well designed to have multi-functions including: (1) thermo-responsive poly(N-isopropylacrylamide) (PNIPAAm) serving as a drug reservoir with a temperature-triggering mechanism, (2) thiolactone moiety for covalent grafting with MNP surface and tuning degree of hydrophobicity of the copolymer, and (3) positively charged poly(N,N-diethylamino-2-ethylmethacrylate) (PDEAEMA) for improving its water dispersibility and ionic adsorption with anionic bio-entities. PNIPAAm responded to the change of the environmental temperature due to the phase separation when crossing its lower critical solution temperature (LCST = 30–34 °C) (Gandhi et al. 2015). When raising the temperature above its LCST, the copolymer was in the collapse state due to the formation of the intramolecular hydrogen bonding among the polymer chains. In contrast, it swelled at the temperature below its LCST owing to the intermolecular hydrogen bonding between water molecules and polymer chains (Du et al. 2010; Bischofberger and Trappe 2015; Patil and Wadgaonkar 2017; Rodkate and Rutnakornpituk 2016; Meerod et al. 2015).

The reactions involving thiol chemistry have now gain a great attention because thiols (-SH) are highly reactive nucleophiles for the reactions with epoxide, alkyl halides, and double or triple bonds (Espeel and Du Prez 2015; Stamenovi et al. 2011). However, the applications of thiols are rather limited because they have a short shelf life due to the oxidation reaction resulting in disulfide formation (Espeel et al. 2012). A promising approach to overcome this limitation is to use a reactive thiolactone, a cyclic thioester, as a latent thiol functional group. This reaction involves a ring-opening reaction of thiolactone moieties to obtain thiol functionality (-SH), subsequently reacting with electrophiles for the second modification in one-pot reaction (Espeel and Du Prez 2015; Chen et al. 2014; Reinicke et al. 2013; Espeel et al. 2011). Many works from Du Prez's research group have reported the use of thiolactone for the double modification purpose (Espeel and Du Prez 2015; Stamenovi et al. 2011; Espeel et al. 2012; Chen et al. 2014; Reinicke et al. 2013; Espeel et al. 2011).

In this report, we describe a synthesis of a thermoresponsive multifunctional diblock copolymer containing thiolactone acrylamide (TlaAm) units for coating on MNP surface and its use for drug-controlled release and bio-conjugation applications. PDEAEMA synthesized via RAFT polymerization was used as a macro chain transfer agent (CTA) for a chain extension of PNIPAAm-*st*-PTlAm second block. PTlAm units were ring opened by alkyl amines to form thiol groups, which were subsequently reacted with the acrylamide-coated MNP to obtain the copolymer-coated particle. PDEAEMA block was then quaternized to obtain cationic MNP to improve the water dispersibility of the particle and for ionic adsorption with negative bio-entities. The effect of alkyl chain lengths (C3, C8, and C12) on the assemblies of the copolymer-coated MNP, affecting their water dispersibility and magnetic separation ability, was investigated. Moreover, the temperature change and the effect of alkyl chain lengths on the rate of the drug release (doxorubicin as a model drug) were also studied (Fig. 1).

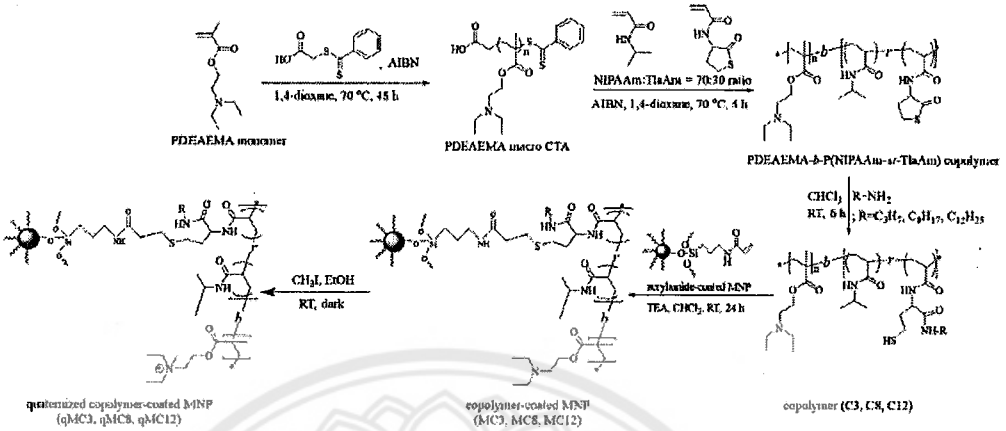

Fig. 1 Synthetic scheme of the copolymer-coated MNP (MC) and its quaternization (qMC)

Experimental

Materials

Unless otherwise stated, the reagents were used without purification: iron(III) acetylacetonate ($Fe(acac)_3$, 99%, Acros), aminopropyltriethoxysilane (APTES, 99%, Acros), *D,L*-homocysteine thiolactone hydrochloride (99%, Acros), oleic acid (Carlo Erba), (3-aminopropyl) triethoxysilane (APTES, 99%, Acros), triethylamine (TEA, 97%, Carlo Erba), 2,2′-azobis(2-methylpropionitrile) (AIBN, 98%, Sigma-Aldrich), s-(thiobenzoyl) thioglycolic acid as a chain transfer agent (99%, Aldrich), 2-(diethylamino) ethyl methacrylate (DEAEMA, 99% stabilized, Acros), and *N*-isopropylacrylamide (NIPAAm, 99%, Acros) were used as received. Acryloyl chloride was synthesized prior to use via a chloride exchange reaction between acrylic acid (98%, Acros) and benzoyl chloride (99%, Acros) to obtain a colorless liquid with 60% yield. 1-Propylamine (99%, Sigma-Aldrich), 1-octylamine (99%, Merck), 1-dodecylamine (98%, Acros), and iodomethane (2.0 M in tert-butyl methyl ether, Sigma-Aldrich) were used as received. Doxorubicin hydrochloride (DOX, 2 mg/ml, Pharmachemie BV) were used as received.

Synthesis of N-thiolactone acrylamide (TlaAm) monomer (Reinicke et al. 2013)

To the mixture of *D,L*-homocysteine thiolactone hydrochloride (7.05 g, 45.6 mmol) in a H_2O/1,4-dioxane solution (100 ml), $NaHCO_3$ (19.20 g, 227.9 mmol) was added and stirred for 30 min in an ice bath. Acryloyl chloride (8.3 g, 91.2 mmol) was then added dropwise and stirred at room temperature overnight. After the reaction completed, brine (100 ml) was added into the solution, followed by extracting with ethyl acetate (3 × 200 ml) to obtain TlaAm in an organic layer. Finally, TlaAm monomer was purified by recrystallization from CH_2Cl_2 and then dried in vacuo.

Synthesis of acrylamide-coated MNP

MNP was synthesized via a thermal decomposition method of $Fe(acac)_3$ (5 g, 14.1 mmol) in 90 ml benzyl alcohol at 180 °C for 48 h. Then, the particle was magnetically separated and washed with ethanol and then chloroform. Oleic acid (4 ml) was slowly added to the MNP-toluene dispersion (30 ml) with sonication to form oleic acid-coated MNP, followed by an addition of APTES (4 ml) containing TEA (2 ml) to form amino-coated MNP. After stirring for 24 h, the particles were precipitated in ethanol and washed with toluene. After re-dispersing the particles (0.1 g) in a NaOH solution (6.72 mmol in 10 ml DI), acryloyl chloride (3.36 g, 37.1 mmol) was then added to the dispersion and stirred for 24 h. The product was magnetically separated, repeatedly washed with water, and then stored in the form of dispersions in THF (0.1 g MNP/1 ml).

Synthesis of PDEAEMA macro chain transfer agent (PDEAEMA macro CTA)

DEAEMA monomer (1.9361 g, 10.4 mmol), S-(thiobenzoyl) thioglycolic acid (31.7 mg, 0.1 mmol) as CTA, and AIBN initiator (4.9 mg, 0.03 mmol) ($[DEAEMA]_0$:[CTA]:[AIBN] molar ratio of 70:1:0.2, respectively) were dissolved in 1,4-dioxane (7 ml) under N_2 atmosphere with stirring for 30 min. The RAFT polymerization was performed for 48 h at 70 °C to obtain ca. 50% monomer conversion with $\overline{M_n}$ of PDEAEMA about 6700 g/mol (Supplementary material Fig. S1). The polymerization was ceased by cooling at room temperature in air. The PDEAEMA macro CTA was purified by dialysis in methanol and dried in vacuo.

Synthesis of PDEAEMA-b-P(NIPAAm-st-TlaAm) block copolymer

PDEAEMA macro CTA (0.06 mmol), NIPAAm (4.24 mmol), TlaAm (1.82 mmol), and AIBN initiator (0.01 mmol) ($[NIPAAm]_0$:$[TlaAm]_0$:[PDEAEMA macro CTA]:[AIBN] molar ratio of 70:30:1:0.2, respectively) were dissolved in 1,4-dioxane (8.5 ml) under N_2 atmosphere with stirring for 30 min. The RAFT polymerization was performed at 70 °C for 4 h to obtain ca.50% NIPAAm conversion and 30% TlaAm conversion with $\overline{M_n}$ of the copolymer about 12,200 g/mol (Supplementary material Fig. S2). The polymerization was stopped by cooling at room temperature with air. The copolymer was purified by dialysis in methanol and dried in vacuo.

Synthesis of the copolymer-coated MNP by a double modification of PDEAEMA-b-P(NIPAAm-st-TlaAm) copolymer

The copolymer (0.16 mmol of TlaAm unit) was dissolved in chloroform (5 ml) followed by an addition of primary alkylamines (0.32 mmol, 2:1 M ratio of alkyl amine to TlaAm unit), e.g., 1-propylamine, 1-octylamine, and 1-dodecylamine, to obtain the C3, C8, and C12 copolymers, respectively. The solution was then mixed with the acrylamide-coated MNP (100 mg) and TEA (0.1 ml) and stirred for 24 h under N_2 gas. The copolymer-coated MNP was magnetically separated and washed with chloroform and designated as MC3, MC8, and MC12, respectively.

Quaternization of PDEAEMA in the copolymer-coated MNP

The copolymer-coated MNP (1.76 mmol of DEAEMA units) was re-dispersed in ethanol (40 ml), followed by dropwise addition of 2 M CH_3I solution (1.76 mmol). The mixture was stirred for 20 h in dark at room temperature. The quaternized products (qMC3, qMC8, and qMC12) were magnetically separated and washed with THF to remove an excess of CH_3I, followed by drying in vacuo to obtain black powder.

In vitro release studies of entrapped DOX from the copolymer-coated MNP

The drug solution (2 mg/ml of DOX) was added dropwise into the quaternized MNP dispersions (10 mg/2 ml in DI water) with stirring at 15 °C for 3 h. The DOX-entrapped MNP was separated from an excess DOX by magnetic separation for 30 min and washed with DI water for 4 times. The dispersion of DOX-entrapped MNP (10 mg in 3 ml DI water) was placed in a water bath at 25 °C (below LCST of PNIPAAm) for 1 h, and then, temperature was increased to 45 °C (above LCST of PNIPAAm) for another 80 min. During the experiment, 0.2 ml of the dispersions was withdrawn from the release media at a predetermined time until the released drug reached the equilibrium (the total time points ranging between 12 and 15). After 30-min magnetic separation, the concentrations of the released drug in the supernatant at a given time were determined via UV-visible spectrophotometry at $\lambda = 480$ nm and % drug release was calculated from the following equation;

$$\%\text{drug released} = \frac{\text{Weight of released drug at a given time}}{\text{Weight of the entrapped drug in the MNP}} \times 100$$

where the weight of the entrapped drug in the MNP was determined from the amount of the drug at the maximum point of the release profile combined with those remaining in the particles. To dissolve the remaining drug from the MNP, DI water (3 ml) was added to the particles and then the mixture was heated at 50 °C for 1 h. After 30-min magnetic separation, the drug concentration in the supernatant was then determined via UV-

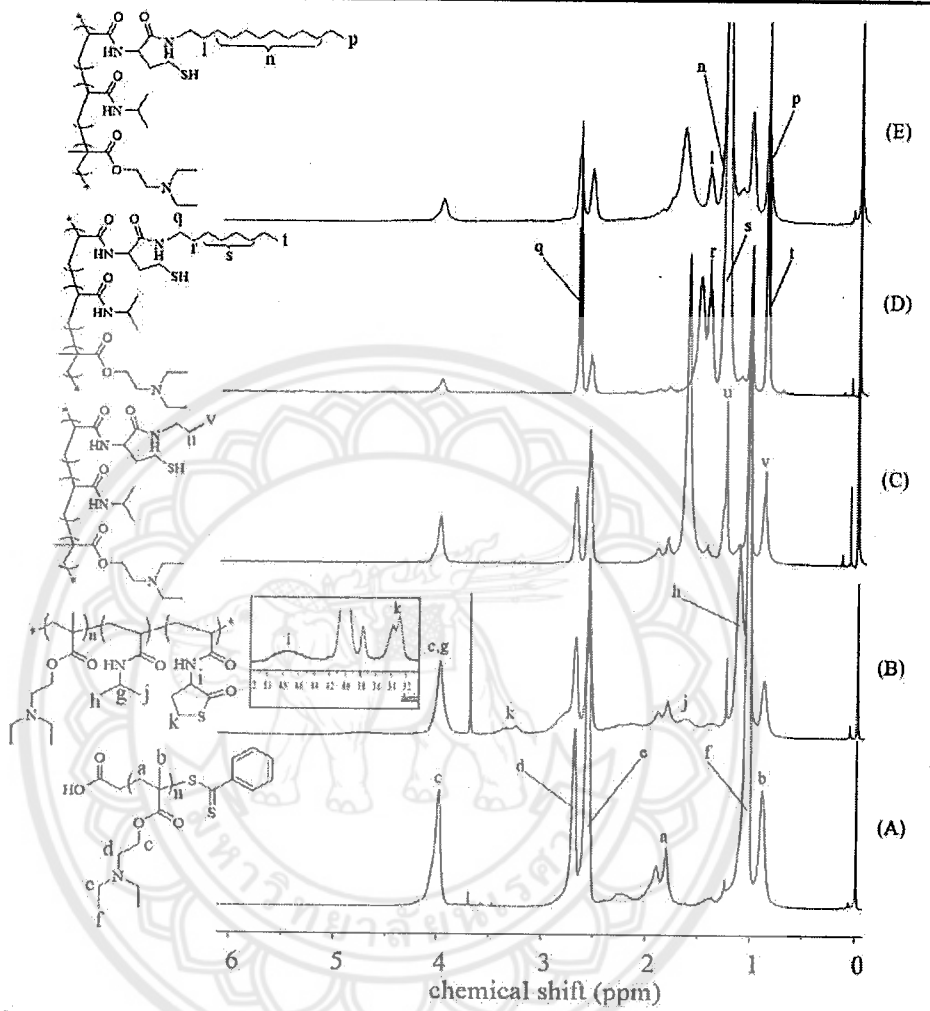

Fig. 2 ^{1}H NMR spectra of a PDEAEMA macro CTA, b PDEAEMA-*b*-P(NIPAAm-*st*-TlaAm) copolymers before the ring-opening reaction, and after the ring-opening reactions with c 1-propylamine, d 1-octylamine, and e 1-dodecylamine

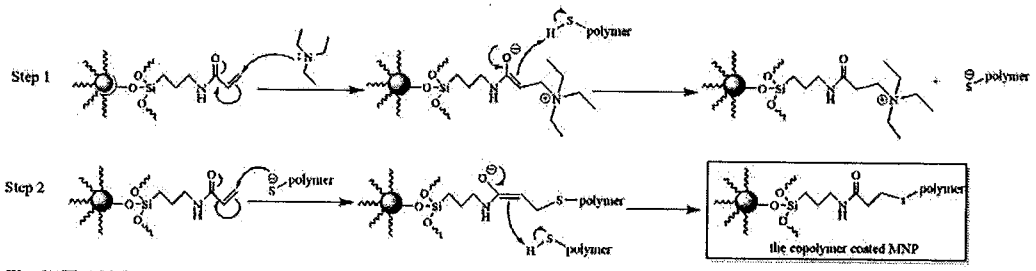

Fig. 3 The thiol-ene reaction mechanism between the acrylamide groups on the MNP surface and thiol groups of the copolymer

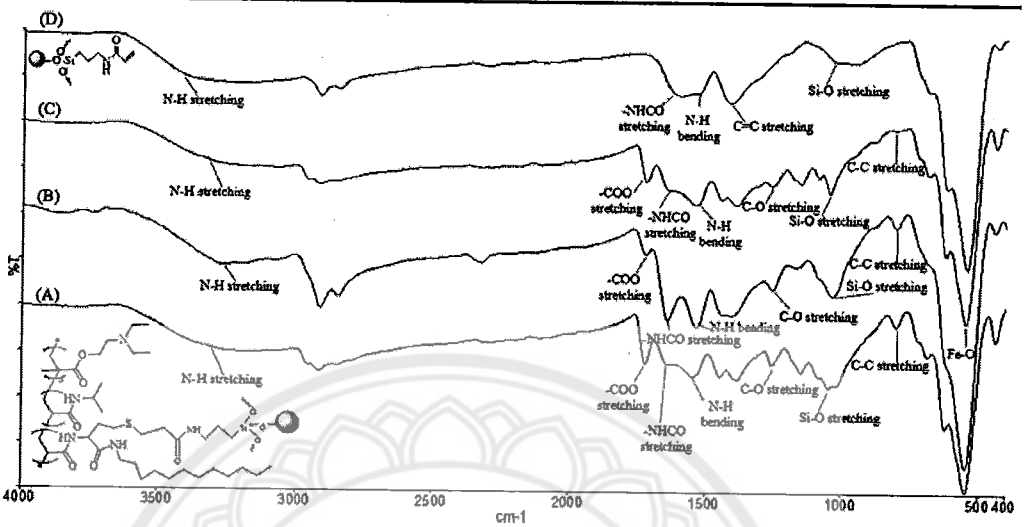

Fig. 4 FTIR spectra of a acrylamide-coated MNP, b MC3, c MC8, and d MC12

visible spectrophotometry. The drug entrapment efficiency was calculated from the following equation:

$$\text{Entrapment efficiency (\%EE)} = \frac{\text{weight of the entrapped drug in the MNP}}{\text{weight of the loaded drug}} \times 100$$

Characterization

FTIR spectrophotometry was operated on a Perkin–Elmer Model 1600 Series FTIR spectrophotometer. ^{1}H NMR spectroscopy was performed on a 400-MHz Bruker NMR spectrometer using DMSO-d_6 or $CDCl_3$ as solvents. The hydrodynamic diameter (D_h) and zeta potential of the particles were measured by PCS using NanoZS4700 nanoseries Malvern instrument. The sample dispersions were sonicated for 1 h before each measurement without filtration. The TEM images were conducted using a Philips Tecnai 12 operated at 120 kV equipped with Gatan model 782 CCD camera. The particles were re-dispersed in water and then sonicated before deposition on a TEM grid. TGA was performed on Mettler-Toledo's SDTA 851 at the temperature ranging between 50 and 800 °C and a heating rate of 20 °C/min under oxygen atmosphere. Magnetic properties of the particles were measured at room temperature using a Standard 7403 Series, Lakeshore vibrating sample magnetometer (VSM). UV-visible spectrophotometry was performed on microplate reader at $\lambda = 480$ nm.

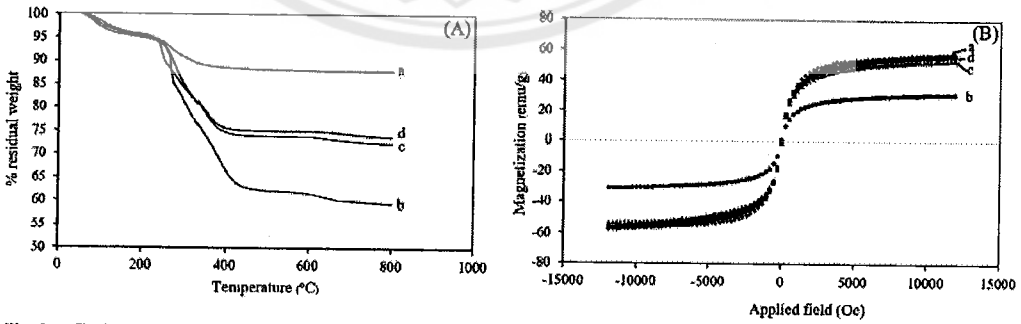

Fig. 5 A TGA thermograms and B *M-H* curves of (a) acrylamide-coated MNP, (b) MC3, (c) MC8, and (d) MC12

Table 1 Zeta potential values and hydrodynamic size (D_h) of the copolymer-coated MNP

Types of MNP	Zeta potential [mV]		D_h of quaternized particles [nm]	
	Before quaternization	After quaternization	at 25 °C	at 45 °C
Acrylamide-coated MNP	−15.3 ± 0.5	−15.3 ± 0.5	564 ± 63	506 ± 52
MC3	0	28.4 ± 1.0	1068 ± 197	396 ± 58
MC8	0	16.2 ± 0.6	836 ± 214	372 ± 103
MC12	0	26.3 ± 0.8	1426 ± 218	295 ± 0

Results and discussion

This work focused on the surface modification of MNP with multi-functional PDEAEMA-*b*-P(NIPAAm-*st*-TlaAm) copolymer to obtain magnetic nanocluster with thermo-responsive properties for drug-controlled release application. The copolymer was synthesized via RAFT polymerization to control architecture and the molecular weight of the block copolymer. PDEAEMA macro CTA was first synthesized, followed by the extension of P(NIPAAm-*st*-TlaAm) second block from PDEAEMA first block. It was envisioned that the quaternized PDEAEMA could form the corona, while P(NIPAAm-*st*-TlaAm) block self-assembled to be a core in aqueous media. (Supplementary material Fig. S3). PTlaAm in the P(NIPAAm-*st*-TlaAm) allowed for a double modification for (1) adjustment of the degree of the hydrophobicity of the polymeric core and (2) immobilization of the polymer on MNP surface. This P(NIPAAm-*st*-TlaAm) core was also used for entrapment of a therapeutic drug with a thermo-triggering release mechanism owing to the existence of PNIPAAm

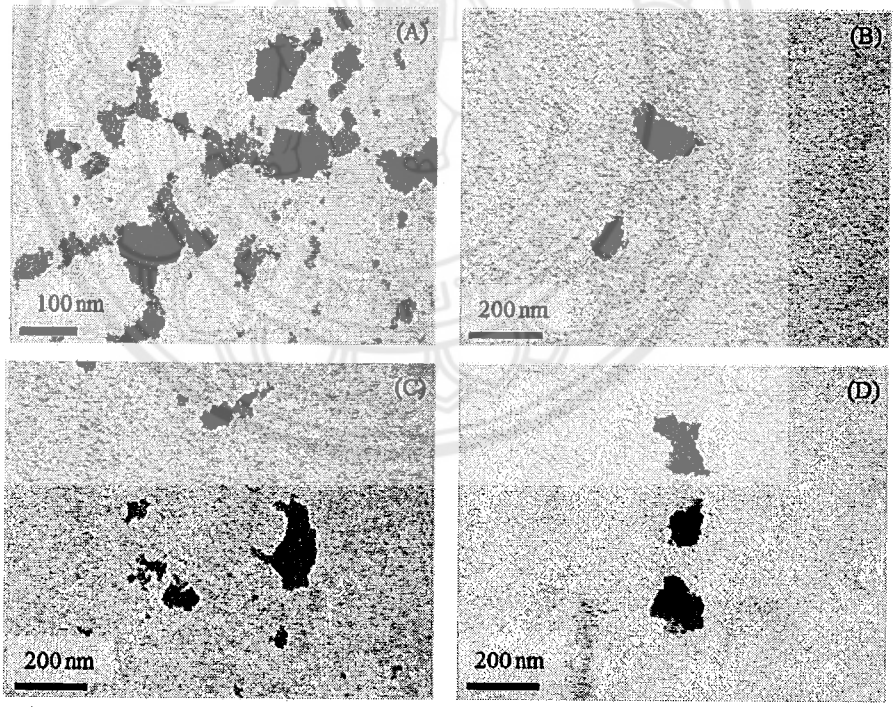

Fig. 6 TEM images of a acrylamide-coated MNP, b qMC3, c qMC8, and d qMC12 prepared from aqueous dispersions

in the structure. In addition, an optimal degree of hydrophilicity/hydrophobicity of the copolymer might be necessary for controlled release of the entrapped drug. Therefore, three different alkyl chain lengths (C3, C8, and C12) were used for tuning the degree of the hydrophobicity of the copolymer coated on the particle surface.

Synthesis and characterization of the copolymer-coated MNP

^{1}H NMR spectra of the purified products from each step are shown in Fig. 2. The signals corresponding to the methylene protons of PDEAEMA macro CTA (1.8–1.9 ppm) indicated the polymerization of PDEAEMA (Fig. 2a). This macro CTA was then used for the propagation of NIPAAm and TlaAm monomers. The new signals at δ 1.1 and 3.6 ppm of the NIPAAm units and at δ 3.2 and 4.7 ppm of TlaAm units indicated the propagation of both monomers from PDEAEMA macro CTA (Fig. 2b). After the ring-opening reactions of thiolactone units with various alkylamines (1-propylamine, 1-octylamine, and 1-dodecylamine), the strong signals of the protons of alkyl groups appeared in the range of δ 0.9–1.4 ppm (Fig. 2c–e). In good agreement with this result, the disappearance of TlaAm signals at δ 3.3–3.4 ppm (signal *k* in Fig. 2b) and δ 4.7 (signal *i* in Fig. 2b), indicating the successful ring-opening reactions of thiolactone moiety in the copolymers. In addition, the results from FTIR were also in good agreement with those obtained from ^{1}H NMR (Supplementary material Fig. S4).

After the ring-opening reaction of thiolactone rings in the copolymers with alkylamines to form thiol groups (-SH), the acrylamide-coated MNP was subsequently added to the mixture allowing for the thiol-ene reaction (Lowe 2010). The proposed thiol-ene reaction mechanism between the acrylamide on the MNP surface and thiol groups (-SH) of the copolymer is shown in Fig. 3. Figure 4 shows FTIR spectra of the acrylamide-coated MNP and the MNP coated with the copolymers after the thiol-ene reaction. The signal at 590 cm^{-1} corresponding to Fe–O bond in the MNP appeared in every sample (Fig. 4). Figure 4b, d shows the characteristic adsorption signals of C=O stretching (1730 cm^{-1}), C–O stretching (1260 cm^{-1}) of carboxyl groups, and C–C stretching (800 cm^{-1}) of the copolymer, signifying the existence of the copolymer on the particle surface through the thiol-ene reaction.

To study the organic/inorganic composition of the copoymer-coated MNP, TGA was used to determine the weight loss at 800 °C (Fig. 5a). It was hypothesized that the residue weight was the weight of iron oxide from oxidized MNP, while the loss weight was the organic conponents in the copolymer-MNP assemblies. The decrease of the residual weight in the samples corresponded to the increase in the organic contents in the MNP. It was found that there was about 12% organic content in acrylamide-coated MNP, while after coating with the copolymer, there were 26, 28, and 41% of the polymers in MC12, MC8, and MC3, respectively, signifying that MC3 had higher degree of alkyl substitution as compared to the other two. This was rationalized that the short alkyl chain length in the C3 copolymer might have less steric hindrance in the particle coating step, resulting in the better accessibility of the particles to react with the copolymers and thus higher amounts of the copolymers on the particles.

VSM technique was used to determine magnetic properties of the MNP before and after the copolymer coating (Fig. 5b). They well responded to an applied magnet and showed superparamagnetic behavior due to the absence of the coercitivity (H_c) and remanence (M_r)

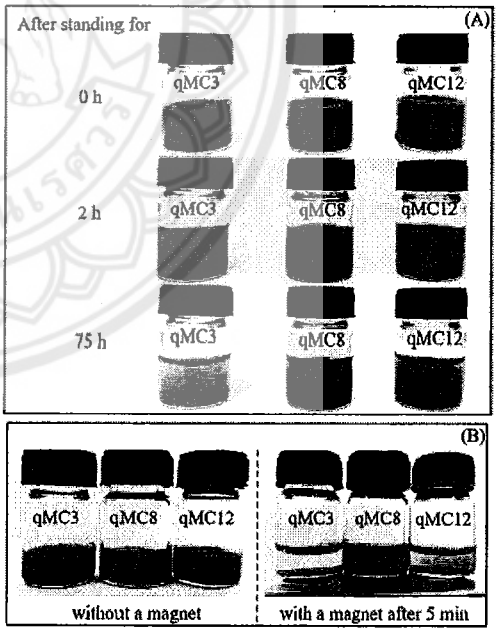

Fig. 7 a Water dispersibility and b magnetic separation ability of qMC3, qMC8, and qMC12

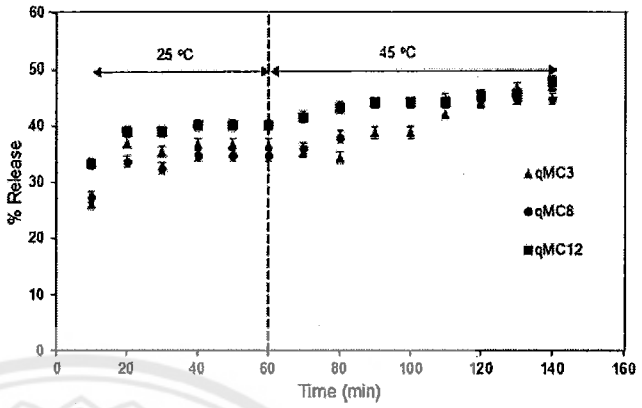

Fig. 8 DOX release profiles of the copolymer-coated MNP (qMC3, qMC6, and qMC12)

upon removal of an external magnetic field. The saturation magnetization (M_s) decreased from 58 emu/g of acrylamide-coated MNP to 56 emu/g of MC12, 54 emu/g of the MC8, and 31 emu/g of MC3, due to the presence of non-magnetic copolymer on the particle surface and thus the drop of their magnetic responsiveness. The decrease in the net magnetization corresponded well to the increase of the copolymers coated on the particles observed in TGA.

The copolymer-coated MNP was then quaternized to improve the particle dispersibility in water. Zeta potentials of the particle both before (MC3, MC8, and MC12) and after quaternization (qMC3, qMC8, and qMC12) were studied using PCS (Table 1). The zeta potentials of acrylamide-coated MNP before and after quaternization did not change because there was no copolymer coated on the MNP surface. After the copolymer coating, their zeta potential values of all copolymers significantly increased from 0 to 16–28 mV after quaternizations, owing to the formation of permanent positive charges of quaternary ammonium groups in the copolymer-coated MNP. It should be noted that these positive charges might facilitate the particles to be well dispersible in an aqueous media, which was necessary for the use in drug-controlled release applications discussed later in this report.

In addition, the preliminary studies in the use of the cationic MNP for ionic adsorption with negative bio-entities were also investigated. DNA tagged with 6-carboxytetramethyl rhodamine (TAMRA-5′-TACC ACCATTC-3′) was selected as a model compound to proof the idea of ionic adsorption capability of the particles. qMC12 (2 mg) as a representative was dispersed in 0.4 μM DNA solution (2 ml) and then stirred for 2 h, followed by magnetic separation. It was found

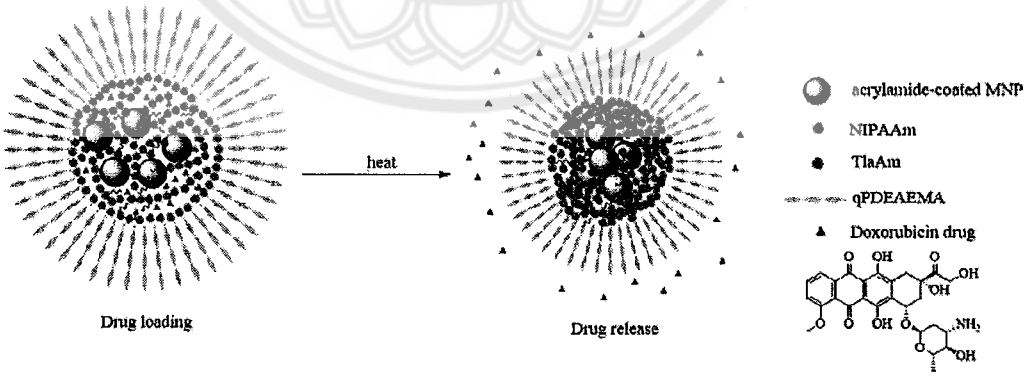

Fig. 9 The proposed mechanism of DOX release from the copolymer-coated MNP

that the concentrations of DNA in the solutions significantly decreased from 0.42 to 0.05 μM (Supplementary materials Fig. S5), indicating that the MNP can be used as a cationic platform for adsorption with DNA through the electrostatic interaction.

Representative TEM images of acrylamide-coated MNP and the quaternized copolymer-coated MNP (qMC) prepared from aqueous dispersions are shown in Fig. 6. Acrylamide-coated MNP showed macroscopic aggregation due to the lack of polymer coating resulting in the particles with poor water dispersibility (Fig. 6a). After coating with the copolymer and then quaternization, formation of the nanoclusters with the size below 200 nm/cluster was observed (Fig. 6b–d). They showed good dispersibility in water without noticeable aggregation after standing for 2 h (Fig. 7a). After 75 h, the qMC3 dispersion exhibited some aggregation, while those of qMC8 and qMC12 were insignificant. This was attributed to the higher degree of alkyl substitution of 1-propylamine in the copolymer due to less steric hindrance as compared to those of 1-octyl and 1-dodecylamines, resulting in the higher degree of hydrophobicity of the copolymer and consequently aggregating in water. The TGA result discussed above also supported this assumption that there was higher amount of the copolymer in qMC3, which might result in the higher degree of hydrophobicity as compared to qMC8 and qMC12.

The particle dispersibility in water shown in Fig. 7a was in good agreement with their magnetic separation ability in water. After 5 min of magnetic separation, qMC3 can be completely separated while there were some dispersible particles remaining in qMC8 and qMC12 dispersions (Fig. 7b). Importantly, the completely separated ability of particles from the dispersion with an assistance of a magnet was necessary for the determination of the drug-controlled release discussed later in this work.

Because the copolymer coated on the particles in this work comprised thermo-responsive moieties of PNIPAAm and PDEAEMA, the effect of the change in the temperature on their D_h was investigated. The experimental temperatures were set at 25 and 45 °C, which crosses their critical solution temperature (LCST of PNIPAAm = 30–34 °C and LCST of PDEAEMA = 31 °C) (Gandhi et al. 2015; Maeda and Mochiduki 2004). It was found that, in all cases, D_h of the particle coated with the copolymers at 45 °C was smaller than those at 25 °C (Table 1). The copolymers collapsed at the temperature above its critical solution temperature, resulting in the shrinkage of the nanocluster and thus the decrease in their D_h. It should be noted that the shrinkage of the copolymer when heated to 45 °C would be utilized as a triggering mechanism for drug-controlled release discussed in the later section.

In vitro release studies of entrapped DOX from the copolymer-coated MNP triggered by the temperature change

DOX, known as a chemotherapy medication used to treat cancer, was used as a model drug for entrapment in and then release from the copolymer-coated MNP. It was hypothesized that DOX was entrapped in the copolymer-coated particles due to the hydrogen bonding of DOX molecules with the copolymer. %EE of qMC3 was ca. 5.4%, while those of qMC8 and qMC12 ranged between 10.3 and 10.8%. The two-fold lower percentage of qMC3 as compared to those of the other two samples was probably due to the higher degree of hydrophobicity in qMC3 (higher degree of alkyl substitution), which might result in less entrapment of DOX on the particles.

DOX release studies were performed at 25 °C with a step-wise increase in the temperature to 45 °C after the equilibrium (Fig. 8). In all cases, the release of DOX from the particle at 25 °C reached their equilibrium within 40 min and they were held at this temperature for 1 h to ensure the equilibrium. Generally, when the temperature of dispersion is increased above room temperature, the preloaded drug should mainly be released via a diffusion mechanism (Liu et al. 2010). In this work, when increasing the temperature to 45 °C (above LCST of PNIPAAm), all samples (qMC3, qMC8, and qMC12) showed the same trend of the drug release. The increment of DOX release upon increasing the temperature was mainly attributed to "a diffusion mechanism". Interestingly, qMC8 and qMC12 showed the faster rate of DOX release with additional release of ca. 8–10% and reached the equilibrium within 40 min. This accelerated release rate was attributed to "a squeezing mechanism" due to the collapse of PNIPAAm chains at above its LCST (Trongsatitkul and Budhlall 2013). However, the release rate of DOX in qMC3 seemed to be retarded at the beginning of the elevated temperature and it was then slowly released afterward with additional DOX release of ca. 11%. The higher degree of hydrophobicity in qMC3 discussed above might inhibit the squeezing behavior of PNIPAAm in the copolymer, which thus initially retarded

the release of the entrapped drug from the particles at the elevated temperature (Fig. 9).

Conclusions

We herein reported the multi-responsive MNP modified with cationic PDEAEMA-*b*-P(NIPAAm-*st*-TlaAm) copolymer and its potential applications in controlled drug release and bio-conjugation. Degree of hydrophobicity of the copolymers coated on surface of particle can be tuned by using various alkyl chain lengths in thiolactone ring-opening reaction and this can influence the particle self-assemblies in water (e.g., D_h, dispersibility, nano-aggregation) and the drug release rate. These particles exhibited the temperature responsive behavior, which can be used as a triggering mechanism for controlled release of DOX. These versatile copolymer-MNP assemblies showed an enormous potential for use as a smart platform with thermal-triggering controlled drug release system and for conjugation with any negatively charged bio-entities.

Acknowledgements The authors acknowledge the Thailand Research Fund (TRF)(RSA5980002) for financial support. MR thanks the National Research Council of Thailand (NRCT) (R2561B086) for the supports. SP thanks The Royal Golden Jubilee PhD Program (PhD/0210/2556) for the scholarship.

Funding This study was funded by The Thailand Research Fund (TRF) (RSA5980002), the National Research Council of Thailand (NRCT) (R2561B086), and the Royal Golden Jubilee PhD Program (PhD/0210/2556).

Compliance with ethical standards

Conflict of interest The authors declare that they have no conflict of interest.

References

Bischofberger I, Trappe V (2015) New aspects in the phase behaviour of poly-N-isopropyl acrylamide: systematic temperature dependent shrinking of PNiPAM assemblies well beyond the LCST. Sci Rep 5:15520–15529

Braunecker WA, Matyjaszewski K (2007) Controlled/living radical polymerization: features, developments, and perspectives. Prog Polym Sci 32:93–146

Chen J-T, Ahmed M, Liu Q, Narain R (2012) Synthesis of cationic magnetic nanoparticles and evaluation of their gene delivery efficacy in Hep G2 cells. J Biomed Mater Res A 100A:2342–2347

Chen Y, Espeel P, Reinicke S, Du Prez FE, Stenzel MH (2014) Control of glycopolymer nanoparticle morphology by a one-pot, double modification procedure using thiolactones. Macromol Rapid Commun 35:1128–1134

Chen L, Zhang H, Li L, Yang Y, Liu X, Xu B (2015) Thermoresponsive hollow magnetic microspheres with hyperthermia and controlled release properties. J Appl Polym Sci 132:42617

Du H, Wickramasinghe R, Qian X (2010) Effects of salt on the lower critical solution temperature of poly (N-isopropylacrylamide). J Phys Chem 114:16594–16604

Espeel P, Du Prez FE (2015) One-pot multi-step reactions based on thiolactone chemistry: a powerful synthetic tool in polymer science. Eur Polym J 6:247–272

Espeel P, Goethals F, Du Prez FE (2011) One-pot multistep reactions based on thiolactones: extending the realm of thiol-ene chemistry in polymer synthesis. J Am Chem Soc 133:1678–1681

Espeel P, Goethals F, Stamenovi MM, Petton L, Du Prez FE (2012) Double modular modification of thiolactone-containing polymers: towards polythiols and derived structures. Polym Chem 3:1007–1015

Gandhi A, Paul A, Sen OS, Sen KK (2015) Studies on thermoresponsive polymers: phase behaviour, drug delivery and biomedical applications. Asian J Pharm Sci 10:99–107

Hill MR, Carmean RN, Sumerlin BS (2015) Expanding the scope of RAFT polymerization: recent advances and new horizons. Macromolecules 48:5459–5469

Hu Y, Meng L, Niu L, Lu Q (2013) Highly cross-linked and biocompatible polyphosphazene-coated superparamagnetic Fe_3O_4 nanoparticles for magnetic resonance imaging. Langmuir 29:9156–9163

Huang L, Liu M, Mao L, Xu D, Wan Q, Zeng G, Shi Y, Wen Y, Zhang X, Wei Y (2017) Preparation and controlled drug delivery applications of mesoporous silica polymer nanocomposites through the visible light induced surface-initiated ATRP. Appl Surf Sci 412:571–577

Leung KCF, Lee S, Wong C, Chak C, Lai JMY, Zhu X, Wang YJ, Wang YXJ, Cheng CHK (2013) Nanoparticle–DNA–polymer composites for hepatocellular carcinoma cell labeling, sensing, and magnetic resonance imaging. Methods 64:315–321

Li Y, Zhang X, Cheng H, Kim G, Cheng S, Zhuo R (2006) Novel stimuli-responsive micelle self-assembled from Y-shaped P(U-Y-NIPAAm) copolymer for drug delivery. Biomacromolecules 7:2956–2960

Lim J, Yeap SP, Che HX, Low SC (2013) Characterization of magnetic nanoparticle by dynamic light scattering. Nanoscale Res Lett 8:381–394

Liu P, Luo Q, Guan Y, Zhang Y (2010) Drug release kinetics from monolayer films of glucose-sensitive microgel. Polymer 51: 2668–2675

Lowe AB (2010) Thiol-ene "click" reactions and recent applications in polymer and materials synthesis. Polym Chem 1:17–36

Machida N, Inoue Y, Ishihara K (2014) Phospholipid polymer-coverd magnetic nanoparticles for tracking intracellular molecular reaction. Trans Mat Res Soc Japan 39:427–430

Maeda Y, Mochiduki H (2004) Hydration changes during thermosensitive association of a block copolymer consisting of LCST and UCST blocks. Macromol Rapid Commun 25: 1330–1334

Mahmoud WE, Bronstein LM, Al-Hazmi F, Al-Noaiser F, Al-Ghamdi AA (2013) Development of Fe/Fe_3O_4 core-shell nanocubes as a promising magnetic resonance imaging contrast agent. Langmuir 29:13095–13101

Matyjaszewski K (2012) Atom transfer radical polymerization (ATRP): current status and future perspectives. Macromolecules 45:4015–4039

Meerod S, Rutnakornpituk B, Wichai U, Rutnakornpituk M (2015) Hydrophilic magnetic nanoclusters with thermoresponsive properties and their drug controlled release. J Magn Magn Mater 392:83–90

Mekkapat S, Thong-On B, Rutnakornpituk B, Wichai U, Rutnakornpituk M (2013) Magnetic core–bilayer shell complex of magnetite nanoparticle stabilized with mPEG–polyester amphiphilic block copolymer. J Nanopart Res 15:2051–2062

Moad G, Rizzardo E, Thang SH (2008) Radical addition fragmentation chemistry in polymer synthesis. Polymer 49:1079–1131

Patil SS, Wadgaonkar PP (2017) Temperature and pH dual stimuli responsive PCL-*b*-PNIPAAm block copolymer assemblies and the cargo release studies. J Polym Sci A Polym Chem 55:1383–1396

Prabha G, Raj V (2016) Preparation and characterization of polymer nanocomposites coated magnetic nanoparticles for drug delivery applications. J Magn Magn Mater 408:26–34

Qin S, Qin D, Ford WT, Resasco DE, Herrera JE (2004) Functionalization of single-walled carbon nanotubes with polystyrene *via* grafting to and grafting from methods. Macromolecules 37:752–757

Qu Y, Li J, Ren J, Leng J, Lin C, Shi D (2014) Enhanced magnetic fluid hyperthermia by micellar magnetic nanoclusters composed of $Mn_xZn_{1-x}Fe_2O_4$ nanoparticles for induced tumor cell apoptosis. ACS Appl Mater Interfaces 6:16867–16879

Reinicke S, Espeel P, Stamenović MM, Du Prez FE (2013) One-pot double modification of P(NIPAAm): a tool for designing tailor-made multiresponsive polymers. ACS Macro Lett 2: 539–543

Rodkate N, Rutnakornpituk M (2016) Multi-responsive magnetic microsphere of poly(N-isopropylacrylamide)/carboxymethylchitosan hydrogel for drug controlled release. Carbohydr Polym 151:251–259

Sahoo B, Devi KSP, Banerjee R, Maiti TK, Pramanik P, Dhara D (2013) Thermal and pH responsive polymer-tethered multifunctional magnetic nanoparticles for targeted delivery of anticancer drug. ACS Appl Mater Interfaces 5:3884–3893

Sciannamea V, Jérôme R, Detrembleur C (2008) In-situ nitroxide-mediated radical polymerization (NMP) processes: their understanding and optimization. Chem Rev 108:1104–1126

Singh LP, Srivastava SK, Mishra R, Ningthoujam RS (2014) Multifunctional hybrid nanomaterials from water dispersible CaF_2:Eu^{3+}, Mn^{2+} and Fe_3O_4 for luminescence and hyperthermia application. J Phys Chem C 118:18087–18096

Stamenovi MM, Espeel P, Van Camp V, Du Prez FE (2011) Norbornenyl-based RAFT agents for the preparation of functional polymers *via* thiol-ene chemistry. Macromolecules 44: 5619–5630

Trongsatitkul T, Budhlall BM (2013) Microgels or microcapsules? Role of morphology on the release kinetics of thermoresponsive PNIPAm-co-PEGMa hydrogels. Polym Chem 4:1502–1516

Ulbrich K, Holá K, Šubr V, Bakandritsos A, Tuček J, Zbořil R (2016) Targeted drug delivery with polymers and magnetic nanoparticles: covalent and noncovalent approaches, release control, and clinical studies. Chem Rev 116:5338–5431

Wang B, Li B, Zhao B, Li CY (2008) Amphiphilic janus gold nanoparticles *via* combining "solid-state grafting-to" and "grafting-from" methods. J Am Chem Soc 130:11594–11595

Wang C, Xu H, Liang C, Liu Y, Li Z, Yang G, Cheng L, Li Y, Liu Z (2013) Iron oxide @ polypyrrole nanoparticles as a multifunctional drug carrier for remotely controlled cancer therapy with synergistic antitumor effect. ACS Nano 7:6782–6795

Willcock H, O'Reilly RK (2010) End group removal and modification of RAFT polymers. Polym Chem 1:149–157